Geophysical Journal International

Indian Plate motion, deformation, and plate boundary interactions

Journal:	*Geophysical Journal International*
Manuscript ID:	Draft
Manuscript Type:	Research Paper
Date Submitted by the Author:	
Complete List of Authors:	Apel, Edwin; University of California, Berkeley, Earth and Planetary Science; AMEC Geomatrix, Geosciences Burgmann, R.; University of California, Earth and Planetary Science Banerjee, Paramesh; Wadia Institute of Himalayan Geology
Keywords:	Planetary tectonics < TECTONOPHYSICS, Neotectonics < TECTONOPHYSICS, Kinematics of crustal and mantle deformation < TECTONOPHYSICS, Continental neotectonics < TECTONOPHYSICS, Continental tectonics: compressional < TECTONOPHYSICS

Geophys. J. Int. (2010) **???**, 1–11

Indian Plate motion, deformation, and plate boundary interactions

E.V. Apel[1] ⋆, R. Bürgmann[1], and P. Banerjee[2]
[1] *University of California, Berkeley Berkeley, California* 94720
[2] *Wadia Institute of Himalayan Geology, Dehra Dun, India*

Received 2009 December 18; in original form 2009 December 22

SUMMARY

We use 1867 GPS-measured velocities to geodetically constrain Indian plate motion and intraplate strain, and we examine plate boundary deformation and plate interactions around the Indian plate. Our solution includes 15 GPS velocities from continuously recording stations from within the stable Indian plate interior that are used to estimate the rotation parameters of the Indian plate with respect to its neighbors. We test a two-plate Indian system divided by the Narmada Son Line and find this scenario to be significant only to 89%. India is a stable continental plate verified by the robust nature of the GPS Data. Dense station coverage along the Himalayan range front allows us to rigorously test boundary parameterizations and develop a preferred plate boundary model. In our preferred model the Himalayan Range Front accumulates ˜50% of the India-Eurasia convergence with as much as 18 mm/yr of slip accumulation along some segments. We compare slip vector orientations with predicted divergence directions from our preferred model along the Somalian plate boundary. We see general agreement between our preferred model and the seismological data. Deviations between our model and the slip vectors highlight areas of diffuse oceanic deformation along the plate boundary. We estimate convergence vectors for the relative plate pairs along the Sumatra subduction zone. We test for the transition between Australian plate convergence and Indian plate convergence along the Sumatra subduction zone and refine the interseismic motion of the Burman sliver plate.

Key words: Plate motions; Space geodetic surveys; Neotectonics

1 INTRODUCTION

The Middle and Far East (centered around India) are a complex region of actively deforming plate boundary zones. With the exception of some discrete mid-ocean ridges in the western Indian Ocean, the Indian plate is bounded by zones of broadly distributed active deformation. The most widely distributed plate boundary in the world is actively deforming as continental India continues to collide with Eurasia. Beginning at the Indian plate's northern edge, along the Himalayan Range Front, active deformation extends through Tibet and into China, Mongolia, and as far north as Russia. Along India's eastern flank the subduction of the Indian plate under the Burma plate in the Andaman-Nicobar Islands region was the source area of most of the 2004 Mw 9.2 Sumatra earthquake rupture. To the south the transition between the Indian plate and the Australian plate is uncertain as seismicity is dispersed over thousands of kilometers and shows no distinct trends that highlight an obviously distinct boundary. Along India's western plate boundary, the Central Indian Ridge, the Carlsberg Ridge, and Owens Fracture zone discretely separate the Indian plate from the Somalian and Arabian plates through a series of spreading centers and transform faults manifested clearly in seismicity trends and bathymetry (Figure 1). It has been difficult to rigorously characterize the kinematics of many of these active boundaries due to the lack of robust Indian plate motion parameters and the complex kinematics of smaller microplates involved in the deformation. Using a comprehensive GPS velocity field of 1867 stations we determine the motion of India with respect to its neighbors, quantify deformation within the Indian plate, and explore the magnitude, nature, and distribution of deformation along the plate boundaries of the Indian plate. We focus on illuminating the pattern of deformation across some of the diffuse plate boundary zones within the context of simple block models that use measured interseismic GPS velocities to estimate the rotations of rigid blocks and elastic strain fields near locked block-boundary faults.

1.1 Geologic Plate Motions

Conventionally, instantaneous Indian plate motion has been estimated using closed plate circuit models and summing motions across mid-ocean ridges constrained by magnetic lineations, transform fault strikes, and earthquake focal mechanisms (DeMets *et al.*, 1990, 1994). In more recent revisions to the plate circuit models DeMets *et al.*, (2005) and Royer *et al.*, (2006) separate Soma-

⋆ Now at: AMEC Geomatrix, 2101 Webster St. Oakland, CA 94612, USA
E-mail: trey.apel@amec.com

lia from Nubia (formally the African plate) reducing the predicted India-Eurasia convergence rates by ˜12% from previous estimates that include Nubia and Somalia as one single plate. Indian plate motion slowed between 20 Ma to 10 Ma as the Himalayas and Tibetan plateau grew and appears constant since ˜8 Ma (DeMets 2005; Merkouriev and DeMets, 2006) . The updated plate motion models more closely match geodetic plate motion estimates derived from GPS measurements (discussed in section 1.2).

1.1.1 Driving Forces

Likely forces that drive Indian plate motion are edge forces (ridge push and slab pull) and basal tractions from relative motions with respect to the underlying mantle at the base of the plate (Cloething and Wortel, 1985; Copley *et al.* 2009, inpress). The gravitational potential of the Tibetan Plateau may also play an important resisting role to northward motion of India (e.g., Flesch *et al.*, 2001; Copley *et al.*, 2009, inpress). In this paper we examine plate boundaries where these forces act and rigorously characterize the plate boundary interaction and deformation. The style and magnitude of the deformation has implications for potential plate tectonic driving forces, particularly in areas of diffuse oceanic deformation (Figure 2) or areas of diffuse continental deformation (Tibetan Plateau) where plate boundaries are not well characterized.

A number of models in recent years have attempted to explain the observed GPS velocities within the Eurasia-India collision zone. End member models include continuum interpretations (e.g. England and Molnar, 2005) and rigid block models (e.g. Thatcher, 2007; Meade, 2007), however discriminating one from the other still remains somewhat of a challenge. Although we adopt the block modeling methods for model parameterization in Tibet we do not assume that it is a unique method for characterizing the deformation observed in the GPS velocities. This is, in large part, due to the fact that the scope of this analysis and paper is focused on describing the deformation (rate and sense of slip) of the upper crust with respect to plate kinematics. We do not attempt to address the full problem of relating the inferred kinematics of fault-bounded crustal blocks to the underlying dynamics and driving forces (Flesch *et al.*, 2001; Copley *et al.*, 2009, inpress)

Surface geodesy (GPS) has been used in an attempt to quantitatively relate crustal deformation to the forces that drive it. However, it requires simplifying assumptions to be made about the strength distribution in the lithosphere. If elastic crust is strongest, interactions among blocks control of deformation. If ductile lithosphere is stronger than flow properties determine the surface deformation. Careful kinematic characterization of deformation in the Indian Ocean and in the Tibetan Plateau may help elucidate the major contributing driving forces of diffuse tectonic deformation.

1.2 Geodetic Plate Motions

Recent geodetic estimates of Indian plate motion (e.g., Paul *et al.*, 2001; Sella *et al.*, 2002; Prawirodirdjo *et al.*, 2004; Socquet *et al.*, 2006a; Bettinelli *et al.*, 2006) used GPS velocity vectors to calculate a pole of rotation that suggests Indian-Eurasian convergence rates are ˜10 % slower than geologic estimates spanning the last 3 Ma (Royer *et al.* 2006). The geodetic location estimates vary (Table 1), in part because data from only two continuous Indian GPS sites (IISC, HYDE) were used. For example, Socquet *et al.*, (2006a) estimate an India-Eurasia geodetic pole using these two sites in addition to four stations in southern Nepal (MAHE, NEPA, BHAI, and SIMR) which they assume record velocities representative of rigid Indian plate motion. Their predicted India-Eurasia convergence rates are ˜5 mm/yr slower along the Himalayan front than those presented in Paul *et al.*, (2001), who also used data from 12 campaign GPS stations distributed across the southern subcontinent. Kogan and Steblov (2008) use DGAR, DHAK and MALD in addition to IISC and HYDE to define stable Indian plate motion. They assign DGAR, which is located close to the India-Australia plate boundary zone to the Indian plate, which does not change their plate motion parameters to a significance level of 95%. Their estimates for IND-EUR plate motion are in good agreement with previously published geodetic poles (Figure 4). In this paper, we incorporate new data (Banerjee *et al.*, 2008) spanning a larger portion of the ”stable” Indian plate than previous studies. Our solution includes data from 29 continuously recording stations in India, including 15 that are located well within the Indian plate. The new data provide robust constraints for estimating plate boundary motion between India and its neighboring plates.

1.3 India Intraplate Deformation

Intraplate seismicity exists across central India. It may be related to flexure of the plate as it is thrust below Tibet (Bilham *et al.*, 2003), high compressive stresses adjacent to the India-Eurasia collision zone, or, in the case of the Mw 7.7 Bhuj earthquake, an extension of diffuse plate boundary deformation that extends from the western Sulaiman range bounding India to the northwest (Stein *et al.*, 2002). The Narmada-Son lineament through central India shows high heat flow and strain rates estimated from seismicity larger than many stable continental regions that may suggest a concentration of intraplate deformation (Rao, 2000) or the separation of India into two distinct plates. It is possible that the seismicity in the region is also enhanced by a thinned and weakened lithosphere due to passive-margin normal faulting in the Cretaceous (Biswas *et al.*, 2007) and by heating from the plume head responsible for the late Cretaceous Deccan flood basalts (Kennett and Widiyantoro, 1999; Chandrasekhar *et al.*, 2009).Here we thoroughly evaluate geodetic evidence of active intraplate deformation within the Indian plate interior from the GPS data.

The Shillong plateau in Northeast India exhibits considerable north-south shortening supported by the existence of large earthquakes such as the great Assam earthquake of 1897 (Bilham and England, 2001). In addition detailed analysis of moderate earthquakes in the same region is also consistent with the north-south shortening (Angelier and Baruah, 2009). Exhumation rates deduced from low-temperature chronometric data suggest a convergence rate of 1-3 mm/yr across the plateau, since 9 Ma (Biswas *et al.*, 2007; Clark and Bilham, 2008). GPS data in the Shillong Plateau region also show contraction with respect to stable India (Banerjee *et al.*, 2008). We separate the Shillong Plateau from India as its own microplate and test its statistical significance using F-statistics. We use the Shillong block’s rotational parameters to estimate slip rates along its boundaries.

1.4 Our Analysis

We present, for the first time, a robust Indian plate model that includes high quality GPS data from within the Indian continent and across its plate boundaries that is well distributed spatially (Banerjee *et al.*, 2008). We model newly processed GPS data and data from published sources (see section 3.2) in a block modeling approach to incorporate both rigid block rotation and a first-order

Table 1. Geodetic Indian Plate Rotation Parameters

Reference	Year	Latitude °N	Longitude °E	Rate ω °/Myr	σ_{maj}	σ_{min}	Azimuth	# Sites Used
Sella	2002	-13.99	53.65	0.483±0.013	11.7	0.5	80	3
Prawirodirdjo	2004	-41.99	45.72	0.487±0.015	12.11	0.73	29	2
Bettinelli	2006	-10.92	51.41	0.483±0.015	NR	NR	NR	5
Socquet	2006	-12.1	50.9	0.486±0.010	5.11	0.61	108	6
THIS STUDY	2010	-1.572	53.27	0.503±0.001	3.144	0.96	86	19

NR - Parameters were not reported.

model of near-boundary elastic strain accumulation effects in a formal inversion of the GPS velocities. We simplify boundary parameters (geometry and locking characteristics) within actively deforming zones in an attempt to constrain motions on large-scale structures without attempting to elucidate the style of deformation (i.e. block-like or fluid-like). The robust plate motion parameters for Eurasia, Australia, Sunda, and India allow for the rigorous testing of variable plate boundary geometries and consideration of models that include smaller microplates within the plate boundary zones. These models allow us to further illuminate patterns in the interseismic strain accumulation along the Indian plate boundary including the Sumatra subduction zone and the Himalayan range front.

2 INDIAN PLATE BOUNDARIES

Tectonic plates are often modeled as rigid blocks with discrete boundaries. Global plate models (e.g., DeMets *et al.*, 1990; Sella *et al.*, 2002) regardless of data source, explain crustal motions well within this simple paradigm. More sophisticated models parameterize plate boundaries, marked by zones of deformation, using a series of rigid blocks with more distributed deformation (typically elastic) occurring along the edges that span the boundary zone (e.g. Meade, 2007). This increased complexity of bounding rigid blocks with elastic dislocations has been useful for interpreting geodetically measured, interseismic crustal deformation data by providing context for far field plate rates while simultaneously estimating slip rates along localized structures.

The Indian plate and its boundaries provide a unique opportunity to fully characterize plate boundary deformation around an entire plate. The collection of geologic slip rates and earthquake sources in and around the Indian plate allow us to compare our model derived from geodetic data with geologic and seismological data in the context of one plate tectonic construct. In the following sections, we will circumnavigate the Indian plate in a counterclockwise direction examining each of the plate boundary deformation zones in turn.

2.1 West: Ocean ridges and transforms

To the west, the Owens fracture zone separates India from the Arabian plate. This fracture zone marks the northernmost oceanic Indian plate boundary. The Owens fracture zone is a dextral transform fault zone (Fournier *et al.*, 2008) that intersects the Makran subduction zone at the diffuse triple junction of the Indian, Arabian, and Eurasian plates. The southern extent of the Owens fracture zone terminates at the India-Arabia-Somalia triple junction. South of the Owens fracture zone, the Indian plate is separated from the Somalian plate along a discrete oceanic rift boundary. This boundary is completely submarine defined by the Carlsberg Ridge and the Central Indian Ridge (Figure 2) highlighted by discrete seismicity (Figure 1), sea floor ridges, young crust, and rift-orthogonal transform faults. Here we compare the orientations of relative plate motions across the oceanic plate boundaries predicted by our model with slip vectors of transform and normal-faulting earthquakes to explore in more detail the transition from Indian to Australian plate motion.

2.2 South: Diffuse India-Australia deformation

Around 6° S, the Carsberg Ridge meets the northern edge of a broad region of oceanic lithosphere that is actively deforming between the adjoining Indian and Australian plates (Wiens *et al.*, 1985) (Figure 1). Delescluse and Chamot-Rooke (2007) thoroughly analyzed this plate boundary zone by exploiting seismological data, far field GPS velocities and heat-flow data, and conclude that the region appears to be neither rigid Indian plate nor rigid Australian plate. They also conclude that while the Ninetyeast Ridge represents a clear strain discontinuity, the separation between the India and Australian plate is not discrete. The broad plate boundary zone (shaded region in Figure 2) may involve an independently rotating Capricorn plate identified from magnetic anomaly data (Demets, *et al.*, 2005 and references therein). As a result the Sumatra subduction zone, south of the Andamans, may mark the edge of either the Indian or Australian plate. We determine an updated pole of India-Australia plate motion to better constrain the regional kinematics across this complex plate boundary zone. As described in sections 2.1 and 2.3, we further explore the distribution of strain in this deformation zone where it interacts with the western and eastern plate boundaries.

2.3 East: Arakan-Andaman- Sumatra

Along the eastern boundary of the Indian plate, south of the Shillong Plateau, is the northwest-southeast striking Arakan Trench and sub-parallel right-lateral Sagaing fault zone. The active Andaman subduction zone is the southern extension of the Arakan Trench that separates the Indian Plate from the Burma microplate. The small, narrow Burma microplate sandwiched between the Indian plate and the Sunda plate (Figure 2) is bounded to the west by the Sumatra subduction zone and to the east by the strike-slip Great Sumatra Fault and its extension of stepping transform and oceanic ridge segments in the Andaman Sea that connect to the Sagaing fault in the north (Curray, 2005). Accurate convergence rates across the Sumatra subduction zone and displacement rates of the Burma microplate are important for recurrence rate estimates in light of the Mw 9.2 Sumatra-Andaman Island earthquake of 2004. The subduction of the Indian or Australian plate under the Burma microplate is the cause for megathrust events like the 2004 earthquake. We update the Sunda and Burma plate motion parameters and interseismic strain accumulation estimates across the Sumatra-Andaman subduction zone. We explore the possibility and implica-

tions of either Indian or Australian plate subduction beneath Sumatra and the effects of both on partitioning between the megathrust and the Great Sumatra Fault.

2.4 North: Himalayan-Tibet

The most notable expression of the Indian-Eurasian plate boundary zone is the Main Frontal Thrust along the Himalayan Range Front. To the east, the frontal thrust appears to terminate in the Eastern Himalayan Syntaxis, north of the Shillong Plateau, as the edge of the Indian plate becomes more distributed (Avouac, 2009). Northward of the Main Frontal Thrust the Indian plate's collision with Eurasia is manifested in the actively deforming Himalayan mountain range and distributed deformation across the adjoining Tibetan plateau (e.g. Tapponnier and Molnar, 1979; Zhang *et al.*, 2004). Estimates of India-Eurasia convergence rates range from 32 to 45 mm/yr from west to east (e.g. Royer *et al.*, 2006; Paul *et al.*, 2001; Sella, *et al.*, 2002) with potentially as much as 20 mm/yr accumulating in the range front itself (e.g. Jade *et al.*, 2004; Lave and Avouac, 2000; Larson *et al.*, 1999). The remainder is distributed to the north across the most diffuse plate boundary in the world. There continues to be much debate about the style of continental deformation in the India-Eurasia collision zone. While one school of thought envisions Tibet to be a thickened, weak and fluid-like zone (e.g., England and Molnar, 2005; Zhang *et al.*, 2004), others consider the tectonics in the region as that of essentially rigid microplates bounded by major lithospheric faults (Replumaz and Tapponnier, 2003; Thatcher, 2007; Meade, 2007). We evaluate the rates of underthrusting along the Himalayas in a block model that allows us to consider the roles of the geometry and locking width of the Himalayan megathrust and the complex kinematics of internal deformation of Tibet. In addition, we consider a Shillong microplate, bounded by the Dauki fault to the north and the Oldham fault to the south, providing the means to more rigorously determine geodetic fault slip rates along its major bounding fault zones and establish the nature and degree of partitioning that the Shillong block imparts on the Himalayan plate boundary.

2.5 Northwest: Transpressional Chaman plate boundary zone

The India-Arabia-Eurasia triple junction marks the transition from diffuse continental deformation to discrete submarine plate boundaries. Active deformation is distributed over a 150km-wide zone accommodating transpressional plate boundary strain across multiple structures. The north-south striking, left-lateral Ornach-Nal and Chaman transform fault zones, and Kirthar thrust belt accommodate Indian-Eurasian plate motion near the coast. Further north the Sulaiman and Salt ranges exhibit similarly diffuse patterns of deformation as they intersect the Main Frontal Thrust of the westernmost Himalayan range. Unfortunately very little GPS data is currently available for this region. As a result we constrain far-field motions but do little to address motion and slip rates along individual small structures across this diffuse region.

3 GPS VELOCITIES

3.1 GPS Data Processing

The GPS data were processed using the GAMIT/GLOBK software package (Herring, 2005; King and Bock, 2005) to solve for station coordinates and velocities in the ITRF2000 reference frame. The primary data come from 106 Survey-mode GPS (SGPS) stations and 29 Continuous GPS (CGPS) stations from India (Banerjee *et al.*, 2008). While the CGPS stations are located all over India including the Himalaya, the SGPS sites are mostly from the northwestern Himalaya. The earliest campaign data were collected in 1995, but most sites were first occupied in 2001. Occupations have been repeated annually through 2007 although some stations have been lost and have been measured for as little as 3 years. Each SGPS station was occupied for 4-6 days continuously, once a year. In addition to the Indian GPS data we also processed data from surrounding IGS stations (IISC, HYDE, KIT3, POL2, LHAS, BAHR, DGAR, MALD, NTUS) available from Scripps Orbital and Positioning Analysis Centre (SOPAC; http://sopac.ucsd.edu). Precise satellite orbits, earth orientation parameters and tightly constrained positions of the IGS sites in a self-consistent reference frame were used to produce daily solutions which include GPS station positions, satellite orbits, earth orientation parameters, and tropospheric delays. The loosely constrained, ambiguity-fixed daily solutions were combined with ambiguity-free quasi-solutions of 33 globally distributed IGS sites (igs1, igs2, igs3), available at SOPAC (http://sopac.ucsd.edu). The local and IGS daily solutions of the entire period were then combined to estimate position and velocities for each site. Selected, globally distributed IGS sites were used to define the ITRF2000 reference frame (Altamimi *et al.*, 2002), both for positions and velocities, with a residual RMS of 3.3 mm and 0.9 mm/yr respectively.

3.2 Published Solutions

In addition to our own analysis we integrated over 2500 GPS-station velocities from published work along the Himalayas, throughout China, Southeast Asia, Australia, Africa and Middle East (Bock *et al.*, 2003; Zhang *et al.*, 2004; Shen *et al.*, 2005; Reilinger *et al.*, 2006; Bettinelli *et al.*, 2006; Socquet *et al.*, 2006a; Calais *et al.*, 2006; Jade *et al.*, 2007; Simons *et al.*, 2007; Sol *et al.*, 2007; Gan *et al.*, 2007; Kogan and Steblov, 2008). Solutions were transformed into a consistent reference frame defined by our original processed solutions. We minimized the misfit (RMS) of collocated stations between networks using a six-parameter transformation (three translations, three rotations). All the transformed velocities remain within 95% confidence level of the original solutions (see Table A1 for site specific details), assuring the robustness of the original solution as well as the transformed one.

3.3 Outlier Exclusion

Some sites were removed from the combined solution and not used in our inversion. Sites were excluded for one of three reasons (see Table A1 for site specific details): 1) We exclude sites outside our area of interest (e.g. Reilinger *et al.*'s (2006) Aegean sites or Gan *et al.* (2007) sites north of the Tarim basin). 2) We exclude sites whose absolute uncertainty exceeds 4 mm/yr. 3) We exclude sites because of extreme misfits to our model. If the residual velocity exceeds 3-sigma then the site was excluded from our inversion. These sites have misfits that deviate from the systematic pattern exhibited by surrounding sites. Some of these sites may have had hardware or site stability problems that did not manifest in the formal velocity uncertainties.

DGAR is included in our velocity combination but is not used to estimate India's rotational parameters. However, the predicted

velocity for the Diego Garcia Island station is consistent with our estimates of Indian plate motion to within ˜1mm/yr (inset Figure 3) similar to Kogan and Steblov (2008). If the DGAR velocity is used in combination with the above mentioned 19 sites to estimate India's rotational parameters the new rotational parameters are statistically indistinguishable from the ones that did not consider the DGAR station. Conversely, a comparison of the DGAR velocity with the predicted velocity using Australian plate parameters is different by ˜6 mm/yr and falls outside of the 2 sigma uncertainty range for residual velocities.

4 METHODOLOGY: PLATES AND BLOCKS

We use a block modeling approach to incorporate both rigid block rotation and near-boundary elastic strain accumulation effects in a formal inversion of the GPS velocities (e.g. McCaffrey *et al.*, 2000; and Meade and Hager, 2005). We consider models that include scenarios with and without independent micro-blocks to constrain the plate rates along the India plate boundaries and elucidate the plate kinematics responsible for interseismic deformation and slip budget estimates.

Plate boundary locations are critical for characterizing GPS velocities and the plate boundary kinematics of a particular region. While some plate boundaries in the Indian region are well defined by active fault traces, youthful geomorphology and abundant local seismicity, others appear more diffuse or the distribution of active deformation may be ambiguous. We draw on the distribution and kinematics of 20th century seismicity, local geology, mapped faults, and the GPS velocity field itself to define our block model boundaries. Most block boundary locations and geometry in our models are based heavily on seismicity trends (e.g. mid-ocean ridges, subduction zone dip) and well recognized plate boundaries (e.g. Himalayan range front). Additional boundary information is adopted or supplemented from plate reconstructions (Replumaz and Tapponnier, 2003) coseismic studies (Pollitz *et al.*, 2006) and prior analyses (Socquet *et al.*, 2006a; Socquet *et al.*, 2006b; Reilinger *et al.*, 2006; Simons *et al.*, 2007; Meade, 2007 and Thatcher, 2007). In some areas, however, geometry is adjusted as indicated by the geodetic data. In the Himalayan and Sumatran regions we test variable geometry for optimal fit (discussed in section 6). Within this paper the term plate (and microplate) refers to the rigid, coherent, lithospheric entity defined by bounding active fault zones. The term block is the specific implementation of these data into a parameterized set of variables within our block model (e.g., Apel *et al.*, 2006).

We implement our blocks as rigid entities on a spherical earth bounded by dislocations and invert for poles and rates of rotation that minimize the misfit to the GPS velocities using the block modeling code by Meade and Hager (2005). The segments that bound the blocks represent uniformly slipping dislocations in an elastic half-space locked to some specified depth (varies by segment, see Table A2 for details). Because our inversion combines rigid block rotation with elastic strain accumulation effects, the parameterization of the block boundary location and geometry is particularly important where the elastic strain field is broadly distributed (such as along subduction zones) and where a large number of stations are located near a boundary fault (such as along the Himalaya frontal thrust).

We invert the horizontal GPS velocities for poles of rotation constrained by the prescribed block locations and geometry defined above. Systematic patterns in the residual velocities (observed minus predicted) are used as an indicator of where and how the model matches the observed surface velocities. Misfit statistics are used to formally evaluate the statistical significance of the block kinematic scenarios we test using the F-test (Stein and Gordon, 1984). For larger blocks (e.g. Eurasia, India, and Arabia) the motion of interior sites are unaffected by plate boundary deformation and effectively define the plate motion parameters. For smaller blocks, elastic strain along the boundaries more directly affects block motion parameter estimates.

4.1 Chi-Squared Statistics

We quantify the goodness of fit in terms of the χ^2 and χ^2/DOF statistics:

$$\chi^2 = \sum_{c=1}^{\#data} \left(\frac{v_c^{model} - v_c^{data}}{\sigma_c} \right)^2 \quad (1)$$

$$\chi^2/DOF = \frac{\chi^2}{\#data - \#model\ parameters} \quad (2)$$

where v_c^{model} and v_c^{data} are the predicted and observed velocity components, and σ_c is the 1σ uncertainty for each component of the input GPS velocities.

The number of degrees of freedom (DOF) is defined by: $\#data$, the number of GPS components used as input data (east and north components for each station) and $\#modelparameters$, the number of model parameters that we solve for in the inversion (3 per block - pole of rotation latitude and longitude and rotation rate). The statistics indicate how well the model fit the data within their uncertainty bounds. Lower values of χ^2 indicate better fit to the data. χ^2 can be calculated for a single data component at a single station, for sites within an individual block, or for the entire model. Increasing the number model parameters inevitably leads to better fits and lower total χ^2. Dividing by the number of degrees of freedom (DOF) helps us to compare our model where we solve for a different number of parameters, but χ^2/DOF ignores all correlations between parameters. Because these correlations change as model geometry changes, caution should be exercised in making strictly quantitative comparisons of models using χ^2/DOF alone. Nonetheless, the statistics provide a basis for qualitative comparisons. For uncorrelated parameters, a χ^2/DOF of 1 indicates that on average all the predicted velocities are consistent with the 1σ standard deviation of the input data.

4.2 *F* Test

Increasing the number of model parameters (i.e. more blocks) inevitably leads to better fits and lower total χ^2 therefore, we use follow the approach of Stein and Gordon (1984) to test the statistical significance of additional microblocks. In our model we test the fit of N motion data (2-component GPS velocities) produced by a model with *b + 1 blocks* for significant improvement relative to a model with *b blocks*. The b block model has *3 (b - 1)* parameters *(N - 3b + 3 degrees of freedom)* while the *b + 1 block* model has *3b* parameters *(N - 3b degrees of freedom)* so the statistic *F*:

$$F = \frac{\chi^2(b\ blocks) - \chi^2(b+1\ blocks)/3}{\chi^2(b+1\ blocks)/(N-3b)} \quad (3)$$

The probability (or 1/significance level) is then calculated given the above mentioned degrees of freedom and the F-statistic. Statistically significant variations are commonly between $\geq$95%.

5 RESULTS: PLATES AND BLOCKS

We evaluate different variations in fault geometry (i.e. location, locking depth, and dip), number of blocks and block configurations in an effort to develop a model that fits the data well while still maintaining geologically reasonable block boundaries locations and geometry. For each variation we inverted the horizontal GPS velocities for poles of rotation and slip rates constrained by our prescribed block locations and plate boundary fault geometry as described in section 2. Systematic misfits remain in some areas, including in our preferred model, as we do not attempt to address every geologic complexity within our study area.

To evaluate the misfit of each block model variation we compare the input GPS velocities with the model's predicted velocities (e.g. Figures 3 and 9). Examining residual velocities (difference between the data velocity and model velocity) allows for a more detailed comparison of the systematic differences between observations and predictions between the different model realizations.

Some block motions are well defined and vary little between our model realizations despite variable block configurations and boundary geometry. The Eurasian block, Australian block, Indian block, and Sunda block's rotational parameters are defined primarily by the sites that lie within the stable interior and are affected very little by plate boundary strain. The inferred motion of smaller blocks, such as the Burma block and smaller blocks within the Himalaya-Tibet region changes based on the parameterization of the boundaries of these blocks. The stability of the major blocks provides robust constraints on far-field motions and allows us to test variable block configurations and deformation geometries along these boundaries used to develop our preferred model.

5.1 India Motion and Deformation

The Indian block's rotational parameters are mostly defined by 19 stations; 3 IGS sites (IISC, HYDE, and MALD), 13 additional CGPS sites (TIR0, KODI, PUN2, BMBY, BHBN, NAGP, JBPR, RRLB, DHAN, JHAN, LUCK, BAN2 and DELH), and 3 sites from previous studies (DHAK from Kogan and Steblov, 2008; COLA and KRN2 from Bettinelli *et al.*, 2006). Previous studies constrained Indian plate motion using only the IGS sites and additional SGPS sites at various locations (e.g. Paul *et al.*, 2001; Socquet *et al.*, 2006a; Bettinelli *et al.*, 2006). The determination of Indian plate motion parameters in earlier studies suffered from a lack of intraplate CGPS stations and narrow east-west aperture of networks within the Indian continent. Our network uses 16 CGPS sites and has good coverage both north-south and east-west providing robust block motion estimates.

5.1.1 Internal Deformation

Residual velocities across India from our inversion (black vectors in figure 3) show systematic northward motion in the south and systematic southward motion in the north. This systematic pattern in the residual velocities suggests unmodeled contraction across central India (Banerjee *et al.*, 2008). We test the significance of a two-block India model using only velocities from the 16 sites processed in our GPS solution. We excluded the 3 sites from other sources (see section 5.1) in an attempt not to model velocity bias from solution combination errors rather than on measureable velocities.

Separation of the Indian block into northern (nIND) and southern (sIND) blocks along a boundary following the Narmada Son line reduces the chi-squared misfit for the 16 sites from 2.06 to 1.59. Our 2-block model predicts contraction that varies from 4 mm/yr in the east to 0 mm/yr in the west near the nIND-sIND pole (Figure 3). The calculated F-statistic (Stein and Gordon, 1984) between the 1-block and the 2-block model is 2.25, equivalent to the 89% confidence level. Because the confidence level is below 95% we chose not to separate India in our preferred model. Although the patterns in the residual velocities indicate an observable systematic change from north to south within the Indian plate, the data do not allow us to determine if the apparent N-S contraction represents broadly distributed intraplate deformation or fragmentation of India into two plates near the Narmada-Son lineament.

5.1.2 Shillong Block Motion

Eleven sites in our GPS solution lie within the boundaries of the Shillong Plateau (Figures 7 and 8). If the sites are included with the above mentioned 16 sites in our Indian plate motion estimates, the reduced chi-squared misfit statistic is equal to 8.05. The reduced chi-squared statistics for those 27 sites decreases to 3.36 when the Shillong block is allowed to rotate independently of India. The calculated F-statistic (Stein and Gordon, 1984) between the two models is 7.23, equivalent to the 99.96% confidence level. Therefore we assume the Shillong block to be independently rotating with respect to India and estimate slip rates along its boundaries (Figure 8). Slip rates predicted from our preferred model (6 mm/yr) along the southern edge of the Shillong block (Dauki fault) are about half of those predicted by Banerjee *et al.* (2008) at 11 mm/yr. Nonetheless, convergence rates along the Main Boundary Thrust along the northern Shillong boundary are higher (˜20 mm/yr) than along the rest of the Himalayan Range Front where slip rates are between 15-18 mm/yr (Figure 8).

5.2 Relative Block Motions

5.2.1 Eurasia

Our Eurasian block's rotational parameters are defined by 19 IGS sites (ARTU, BOR1 BRUS, GLSV, GOPE, HERS, JOZE, KIRU, KOSG, LAMA, MDVO, MOBN, NRIL, NVSK, NYA1, POTS, TIXI, WTZR, and ZWEN.) Misfits are all less than 1.5 mm/yr with a mean misfit of 0.65 mm/yr (inset Figure 4). The EUR plate rotation parameters are very well constrained and consistent with previously published poles shown in Table 2. The consistency of our EUR pole with previously published poles indicates that sites within our EUR block contain little bias.

We compare IND-EUR poles from our one-plate and two-plate models with published poles (Figure 4). In our models it appears that India's plate motion parameters are dominated by the southern sites as our sIND-EUR and IND-EUR poles are statistically indistinguishable. All of the published IND-EUR pole estimates (see references listed in Figure 4 and Table 2) vary significantly in their east-west location due to the primarily north-south distribution of stations. Poles from this study also show larger uncertainties in the east-west direction due to the inherently narrower east-west aperture of the network. However, the magnitude of the uncertainties is 50-80% smaller in this study than in previous work.

5.2.2 Somalia and Arabia

The Somalia block's rotational parameters are defined by 7 sites from Stamps *et al.* (2008) and 6 sites from Reilinger *et al.* (2006). Sites from Stamps *et al.*, (2008) are concentrated mostly in the

southern region of the block while sites from Reilinger *et al.*, (2006) are mostly in the north. The Somalia block rotation is consistent with both Stamps *et al.* (2008) and Reilinger *et al.* (2006) although there is some variation resulting from the combination of the two solutions.

The Arabian block's rotational parameters are defined by 22 sites. All but one of these GPS velocities comes from Reilinger *et al.* (2006). Misfits are all less than 4 mm/yr with a mean misfit of 1.6 mm/yr and a reduced chi-squared statistics equal to 1.5. The lack of systematic patterns in the residual velocities among the well distributed stations within the Arabian block suggest little to no measureable internal deformation.

5.2.3 Australia

The Australian block's rotational parameters are defined by 6 IGS sites (HOB2, JAB1, KARR, PERT, TIDB, and YAR1,) and 4 sites (DARW, CEDU, ALIC, and TOW2) from Bock *et al.* (2003). The mean misfit of 2.0 mm/yr is shown in the inset of Figure 5. These rotation parameters differ from previously published poles (e.g. Sella *et al.*, 2002; Bock et al, 2003; Delescluse and Chamot-Rooke, 2007) in that our relative IND-AUS pole location lies further south than other geodetic poles (Figure 5).

Although Indian plate motion independent of the Australian plate is not a particularly new idea (e.g., Le Pichon, 1968; DeMets *et al.*, 1994), ten GPS velocities within the stable Australian plate precisely discriminate Australian motion with respect to India. Our new solution provides tight constraints on the relative far-field motion and provides context for the proposed Capricorn plate and widely distributed deformation within India's southern plate boundary zone (Delescluse and Chamot-Rooke, 2007).

5.2.4 Sunda

Sunda's rotational block parameters are defined by 49 sites from Bock *et al.*, 2003; Calais *et al.*, 2006; Simons *et al.*, 2007; and Socquet *et al.*, 2006. Three sites from Thailand (Socquet *et al.*, 2006) were excluded from block parameter estimates and our preferred model (but shown on Figure 9) as extreme outliers (see section 3.3). Some sites from northern Borneo were excluded because these sites may move independently of the Sunda block (Simons *et al.*, 2007). All sites east of 119°E were also excluded as we did not attempt to address the complexities in the Sulawesi region. The Sunda block's rotational parameters are statistically compared with previously published poles in Table 2.

6 PLATE BOUNDARY INTERACTIONS

India's relative plate motion drives deformation at its boundaries. We compare predictions of deformation rates and styles from our preferred model along each boundary with geology, geomorphologic features, and seismicity.

6.1 Eurasia

The deformation associated with India's collision with Eurasia is manifested most famously along the Himalayan range front and diffused through the Tibetan plateau. Along the Himalayan Range Front we estimate total IND-EUR convergence to vary from 33-39 mm/yr from ˜76°-91° east longitude. The amount of deformation accommodated on the main Himalayan thrust system depends on the nature and distribution of deformation in southern Tibet. Our Tibetan plateau block geometry is simplified and modified from previous studies (e.g. Meade, 2007; Thatcher, 2007) as this paper does not attempt to address all the complexities of the entire India-Eurasia collision zone. We parameterize the Himalayan front with four main blocks defined by the major geologic features like the Indus-Zangbo suture, Gulu rift, and Karakorum fault (Figure 7).

Slip along the HRF varies from 15-18 mm/yr with the greatest amount in the NE, Bhutan Himalaya north Shillong, and the least in central Tibet (Figure 7). Estimates of slip from our model are consistent but smaller than other published estimates (see Feldl and Bilham, 2006). By separating Tibet into multiple blocks our model captures east-west extension evidenced by predicted slip rates along structures like the Gulu-Sangxung and Kung Co graben systems (Figure 7). Our extension rates (4-9 mm/yr) are quite consistent with other estimates of extension in southern Tibet (e.g. Chen, 2004b) which use considerably fewer GPS data. Differences between the two estimates are the result of block boundary choice and model parameterization.

The Shillong block rotates counterclockwise evidenced by lower slip rates (18 mm/yr) along the Bhutan Himalayas and higher slip rates (25 mm/yr) further to the east (Figure 7). The predicted slip rate along the Dauki fault is 6 mm/yr, or 60% less than the rate estimated by Banerjee *et al.*, (2008), but twice the rate suggested by geologic studies (Biswas *et al.* 2007, Clark and Bilham, 2008). Fit to our model is good (inset Figure 7) although lack of data along the most northeastern extent of Himalayan range north of the Shillong Plateau leaves slip rates poorly constrained in this region.

North of the Makran subduction zone block motion is transferred from the collision of the Arabia to Indian-Eurasian motion (11 mm/y of contraction and 28 mm/yr sinistral) along the Ornach Nal Fault through the Chaman Transform zone and into the Sulaiman Range. However, lack of GPS station density prevents us from making more precise estimates of slip, and our model does not try to capture the complexities of deformation in the zone.

6.2 Somalia

The eastern Somalian plate boundary is quite discrete, separating SOM from the Australian plate along the Central Indian Ridge in the south and from the Indian plate along the Carlsberg Ridge in the north (Figures 2 and 6). Because of the submarine nature of these boundaries we compare our predicted displacement directions (plate vectors) with earthquake slip vectors from events along the spreading centers. We derive slip vectors from focal mechanism solutions (www.globalcmt.org) south of the SOM-IND-ARB triple junction and north of the SOM-AUS-ANT triple junction. We selected only those events between these triple junctions that lie within 100 km of the mid-ocean ridge, which we assume are related to the divergence of the plates. 311 events from the catalog fit our selection criteria. We derive slip vectors for these events and compare them to the azimuth of plate motion calculated from our model at the location of each earthquake (inset rose diagrams in Figure 6).

Along the Somalian plate boundary the relative plate motion transitions from SOM-IND to SOM-AUS block motion through the diffuse India-Australia plate boundary zone (Royer and Gordon, 1997). We attempt to elucidate the diffuse nature of the IND-AUS plate boundary along the mid-ocean ridges by comparing both the predicted SOM-IND plate vectors and the SOM-AUS plate direction with the slip vectors in the central ridge region (12°S-2°N lat).

The trend of the slip vectors in the north along the Carlsberg Ridge are consistent with SOM-IND block motion (top inset Figure 6).

Along the central section of the mid-ocean ridges slip vectors appear more consistent with SOM-IND block motion rather than with SOM-AUS plate motion (middle inset Figure 6). In the central section the orientation of SOM-IND motion and SOM-AUS motion becomes sub parallel because of the close proximity to the IND-AUS pole (Figure 5) making the distinction between the two difficult. The IND-AUS-SOM triple junction remains somewhat enigmatic due to the diffuse nature of the IND-AUS plate boundary. Based on our analysis, we posit that the IND-AUS-SOM triple junction is likely to be on the Carlsberg or Central Indian ridge south Diego Garcia Island. The GPS velocity at DGAR is statistically indistinguishable with respect to stable Indian motion (see section 5.1) it seems likely that DGAR is a part of the Indian plate.

South of 11°S lat nearly all of the slip vectors are exactly parallel with SOM-AUS plate motion with a small concentration of dip slip events that deviate from the plate motion direction. These events are not concentrated spatially and are scatter throughout the southern region from north to south. The correlation between the slip vector data in this region and the plate velocities directions suggest that our SOM-AUS relative plate motion is robust and we see little evidence that indicates that discriminating a Capricorn plate is possible given the GPS and slip vector data.

6.3 Arabia

The Owens Fracture Zone separates the Indian plate from the Arabian plate and accommodates ˜5 mm/yr of dextral motion (see Table A2 for segment specific slip rates), greater than the rate of 3 mm/yr predicted by Demets (2008) and Fournier *et al.*, (2008) and slightly greater than the rate predicted by Reilinger *et al.*, (2006) The rotation of the Arabian block with respect to Eurasia is manifested, as convergence along the Makran subduction zone at 35-38 mm/yr. The rate of subduction may be as little as 23 mm/yr (Reilinger *et al.*, 2006) if an independent Lut block is considered (Figure 2). Unlike Reilinger *et al.*, (2006) we did not include a separate Lut block in our preferred model as it is not required by the currently available data. Possible Lut block motion is only constrained, at present, by 2 GPS sites, both of which are within the zone of elastic strain accumulation of the Makran subduction zone.

6.4 Australia

GPS velocities within the interior of Australia and India clearly show that the two blocks move independently of each other (Figure 5) and verified with F-statistics; however, the tectonic boundary between the two remains enigmatic and may be complicated by an independently rotating Capricorn plate (Demets, *et al.*, 2005 and references therein). The boundary zone between the Indian and Australian plates is quite diffuse (Delescluse and Charmot-Rooke, 2007). Within this zone our preferred model predicts 1-2 mm/yr N-S extension west of the IND-AUS pole between it and the Central Indian Ridge (Figure 5) and up to 12 mm/yr of N-S contraction in the vicinity of the 90°E ridge. The IND-AUS-SOM and the IND-AUS-SUN triple junctions remain somewhat enigmatic due to the diffuse nature of the IND-AUS plate boundary. The refined plate motion parameters of the Indian and Australian plate do little to elucidate these triple junctions. We explore their locations in the following sections.

6.5 Sunda

The interaction between the Sunda plate and the Indian plate is most significant along the Sumatra-Andaman subduction zone where IND-SUN motion is partitioned along the megathrust and the sub-parallel strike-slip Great Sumatra Fault (e.g. McCaffrey *et al.*, 2000). We consider a separate Burma forearc block (sliver block) bounded by the Sumatra subduction zone and the Great Sumatra Fault (Figure 2). Along the Sumatra subduction zone segment, the geometry parameterization is based on previous geometric constructions (e.g. McCaffrey 2002; Banerjee *et al.*, 2007; and Chlieh *et al.*, 2007). Residual velocities from the Sumatra region, while larger than in most other areas do not show any systematic patterns (Figure 9). The few large outliers that do exist (Bettinelli et al, 2006) are related to poorly resolved station velocities rather than model misfits and were excluded from our final analysis (see discussion in section 3.3).

In an attempt to elucidate an optimal boundary location in the zone of diffuse deformation between the Indian and Australian blocks (Figure 2) we migrated our block boundary along the Sumatra subduction zone through the segment endpoints (number 1-11 in Figure 9). We compute and compare the model misfit at each of these segment intersections. We repeated this test while also varying the Sumatra segment geometry (locking depth and dip) to estimate best-fit parameters for the region. In this analysis, we assume homogenous segment parameters for the subduction zone (same dip and locking depth).The relationship between locking depth and dip are directly correlated. As dip increases so too does the locking depth required to minimize the misfit to the GPS velocities. However, our heterogeneous segment parameters fit our data better than any of the homogenous segment geometry sets. Regardless of segment geometry, the segment location with the minimum misfit was endpoint 8 (Figure 11) the approximate southern extent of the 1797 rupture and the extent of significant locking proposed by Chlieh *et al.*, (2007). Interseismic slip rates from our preferred model (18-22 mm/yr) are consistent with published geologic estimates of slip rates along the Great Sumatra Fault (e.g. Sieh and Natawidjaja, 2000) and backarc spreading ridges (Curray, 2005) and provide robust estimates of Burma block motion.

7 DISCUSSION

7.1 Internal Indian Deformation

Systematic differences in the GPS velocities from southern and northern India may reflect internal deformation of the Indian plate. Statistical significance of two separate plates is below 95%, and thus our preferred model assumes a single rigid Indian plate. However, if northern and southern Indian plates exist the GPS velocities predict contraction in central India (Figure 3), concentrated potentially along the Narmada-Son lineament. The Narmada-Son has experienced two major earthquakes (1938 Satpura earthquake and the 1997 Jabalpur earthquake) suggesting that it may be an actively deforming structure (e.g., Rao, 2000).

Intraplate deformation in central India could also result from flexure of the Indian plate as it collides with Eurasia (Bilham *et al.*, 2003). Estimates of localized deformation resulting from flexure are somewhat smaller in magnitude than those predicted from a two plate system, although the flexure also predicts contractional deformation in central India. Bilham *et al.*, (2003) show how flexural deformation may be reflected in the stress field and topography. Our analysis rigorously considered the former model and found that

while some systematic residual velocities are evident when assuming a rigid Indian plate, they are not statistically significant to justify a two-plate system.

7.2 Diffuse Continental Deformation

Although modern GPS data provides robust measurements of displacements rates, interpretations of these data vary, especially in areas of diffuse continental deformation like Tibet. With far field motions of the bounding Indian and Eurasian plates tightly constrained, differences in micro-block rotations and slip estimates along the Himalaya vary mostly as a result of variable data densities, model parameters, and assumptions. Meade (2007) uses a conceptually identical model with fewer GPS stations (Zhang *et al.*, 2004 only). Estimates of slip from Meade (2007) along the HRF vary from 17-22 mm/yr, 15-20% greater than our model. Differences in convergence rates along the HRF may partly be the result of different Indian plate motion parameters, but these differences do not explain a reduction in convergence by 15-20%. Meade's (2007) higher slip rates are the result of a more steeply dipping HRF. In our preferred model segments along the HRF dip between 6 and 8 degrees. We estimate these dips by migrating the HRF boundary from north to south and varying the dip and locking depth exploring ranges of geometries that minimize the misfit to the observed data while maintaining the projection of the bottom locking depth to correspond with the 3500 m topographic contour (Avouac, 2003). Shallower dipping segments require less slip to produce similar magnitudes of elastic deformation at the surface then more steeply dipping segments. As a result our preferred model requires lower slip rates than Meade's (2007) to produce similar fits to the data.

Thatcher (2007) uses the same data (Zhang *et al.*, 2004) and after removing sites "where effects of elastic strain accumulation are large" estimates block rotation rates that are even larger than Meade's (2007). Thatcher's (2007) assumption is that the remaining velocities only capture rigid block motion and that no component of the velocity is measuring elastic strain accumulation. It's not surprising then the block rotation estimates (and fault slip estimates) from this method are larger than those for method's that consider elastic strain effects.

We note that differences in analyses within the same conceptual framework are largely the result of assumptions made within the analyses, whether it's the rigidity of the blocks or the parameters of the segments that bound them. First order results from our model, Thatcher's (2007) and Meade's (2007) all suggest that the paradigm of plate tectonics (i.e. rigid blocks controlling crustal deformation) holds true at large scales and may be appropriate to some degree for continental deformation. Although even in the same family of models, using the same data there still exist discrepancies (geodetic slip rates vs. geological slip rates) that have not yet been adequately addressed and may require a more sophisticated analysis than simple rigid block models, particularly in areas of diffuse deformation like continents.

7.3 India-Australia Plate Boundary

Based on GPS data presented here we estimate robust India-Australia plate motion parameters that constrain far-field motions between the plates. Most of the sites lie within the "stable" interiors of the two plates far away from the submarine boundary between India and Australia. The data themselves do not elucidate the plate boundary or the locations of the IND-AUS-SOM or IND-AUS-BUR triple junctions.

The eastern triple junction (IND-AUS-BUR) is somewhat difficult to constrain. Delescluse and Charmot-Rooke (2007) suggest that the 90°E Ridge is a major discontinuity for both strain and velocity. The intersection of this ridge with the Sumatra-Andaman subduction zone could be the northern most possibility of the triple-junction. However, our modeling suggests (section 5.3.4) that the interaction along Sumatra is much more likely to be Indian plate motion rather than Australian pushing the triple junction location much further south (Figures 9 and 11). Implications of Indian plate motion driving convergence this far south include potential underestimation of long term plate convergence along the Sumatra subduction zone.

Magnetic anomaly analysis (Demets *et al.*, 1994) and seismicity (Royer and Gordon, 1997) indicate a potential western triple junction (IND-AUS-SOM) between 2°-9°S. We place the IND-AUS-SOM triple junction at the southern edge of this zone. Placement of the triple junction this far south (Figure 11) is required so for the DGAR site to be on the Indian plate (see discussion in 5.3.5). However, the ambiguous nature of the triple junction location suggest that an independent Capricorn might be responsible for the deformation observed in the region.

8 CONCLUSIONS

We present robust Indian plate motion rotational parameters. Using numerous GPS sites across India, Eurasia, Australian, Somalia, and Sunda. We refined relative plate motions between the previously mentioned plates and performed a detailed kinematic assessment of India's plate boundary interactions with its adjacent tectonic plates not previously possible given the scarcity of geodetic data within India. The robust nature of the Indian plates' motion is shown through the rigorous testing of intraplate deformation possibilities within the Indian continental interior. We see little to no statistical evidence for intraplate deformation within the Indian plate suggesting that it is appropriate to treat it as a stable tectonic plate.

These very tightly constrained relative plate motions provide a conceptual framework to examine plate boundary deformation. The relative orientation of plate motions at the boundaries can be compared directly with seismicity and recent faulting to examine consistency between geodesy, geology, and seismology and provide insight into the driving forces behind plate boundary deformation. To a first order there's general consistency between our plate tectonic model (i.e block-like) of deformation and additional independent data sets. Discrepancies that may exist are often result of poor data density pore data quality or simplified model assumptions.

ACKNOWLEDGMENTS

We would like to thanks XX for their helpful reviews.

REFERENCES

Allmendinger, R. W., Reilinger, R., & Loveless, J., 2007. Strain and rotation rate from gps in tibet, anatolia, and the altiplano, *Tectonics*, **26**(3).

Altamimi, Z., Sillard, P., & Boucher, C., 2002. Itrf2000: A new release of the international terrestrial reference frame for earth science applications, *Journal of Geophysical Research-Solid Earth*, **107**(B10), 19.

Angelier, J. & Baruah, S., 2009. Seismotectonics in northeast india: a stress analysis of focal mechanism solutions of earthquakes and its kinematic implications, *Geophysical Journal International*, **178**(1), 303–326.

Apel, E. V., Burgmann, R., Steblov, G., Vasilenko, N., King, R., & Prytkov, A., 2006. Independent active microplate tectonics of northeast asia from gps velocities and block modeling, *Geophysical Research Letters*, **33**(11), 5.

Avouac, J. P., 2003. Mountain building, erosion, and the seismic cycle in the nepal himalaya, in *Advances in Geophysics, Vol 46*, vol. 46 of **Advances in Geophysics**, pp. 1–80, Academic Press Inc, San Diego.

Banerjee, P. & Burgmann, R., 2002. Convergence across the northwest himalaya from gps measurements, *Geophysical Research Letters*, **29**(13).

Banerjee, P., Pollitz, F., Nagarajan, B., & Burgmann, R., 2007. Coseismic slip distributions of the 26 december 2004 sumatra-andaman and 28 march 2005 nias earthquakes from gps static offsets, *Bulletin of the Seismological Society of America*, **97**(1), S86–S102.

Banerjee, P., Burgmann, R., Nagarajan, B., & Apel, E., 2008. Intraplate deformation of the indian subcontinent, *Geophysical Research Letters*, **35**(18), 5.

Bendick, R. & Flesch, L., 2007. Reconciling lithospheric deformation and lower crustal flow beneath central tibet, *Geology*, **35**(10), 895–898.

Bettinelli, P., Avouac, J. P., Flouzat, M., Jouanne, F., Bollinger, L., Willis, P., & Chitrakar, G. R., 2006. Plate motion of india and interseismic strain in the nepal himalaya from gps and doris measurements, *Journal of Geodesy*, **80**(8-11), 567–589.

Bilham, R. & England, P., 2001. Plateau 'pop-up' in the great 1897 assam earthquake, *Nature*, **410**(6830), 806–809.

Bilham, R., Bendick, R., & Wallace, K., 2003. Flexure of the indian plate and intraplate earthquakes, pp. 315–329, Indian Academy Sciences.

Biswas, S., Coutand, I., Grujic, D., Hager, C., Stockli, D., & Grasemann, B., 2007. Exhumation and uplift of the shillong plateau and its influence on the eastern himalayas: New constraints from apatite and zircon (u-th-[sm])/he and apatite fission track analyses, *Tectonics*, **26**(6), 22.

Bock, Y., Prawirodirdjo, L., Genrich, J. F., Stevens, C. W., McCaffrey, R., Subarya, C., Puntodewo, S. S. O., & Calais, E., 2003. Crustal motion in indonesia from global positioning system measurements, *Journal of Geophysical Research-Solid Earth*, **108**(B8), 22.

Bollinger, L., Avouac, J. P., Cattin, R., & Pandey, M. R., 2004. Stress buildup in the himalaya, *Journal of Geophysical Research-Solid Earth*, **109**(B11).

Calais, E., DeMets, C., & Nocquet, J. M., 2003. Evidence for a post-3.16-ma change in nubia eurasia north america plate motions?, *Earth and Planetary Science Letters*, **216**(1-2), 81–92.

Calais, E., Dong, L., Wang, M., Shen, Z., & Vergnolle, M., 2006. Continental deformation in asia from a combined gps solution, *Geophysical Research Letters*, **33**(24), –.

Chandrasekhar, D. V., Burgmann, R., Reddy, C. D., Sunil, P. S., & Schmidt, D. A., 2009. Weak mantle in nw india probed by geodetic measurements following the 2001 bhuj earthquake, *Earth and Planetary Science Letters*, **280**(1-4), 229–235.

Chlieh, M., Avouac, J. P., Hjorleifsdottir, V., Song, T. R. A., Ji, C., Sieh, K., Sladen, A., Hebert, H., Prawirodirdjo, L., Bock, Y., & Galetzka, J., 2007. Coseismic slip and afterslip of the great m-w 9.15 sumatra-andaman earthquake of 2004, *Bulletin of the Seismological Society of America*, **97**(1), S152–S173.

Clark, M. K. & Bilham, R., 2008. Miocene rise of the shillong plateau and the beginning of the end for the eastern himalaya, *Earth and Planetary Science Letters*, **269**(3-4), 336–350.

Cloetingh, S. & Wortel, R., 1985. Regional stress-field of the indian plate, *Geophysical Research Letters*, **12**(2), 77–80.

Copley, A., Avouac, J. P., & Royer, J. Y., 2009 (inpress). The india-asia collision and the cenozoic slowdown of the indian plate; implications for the forces driving plate motions, *Journal of Geophysical Research-Solid Earth and Planets*.

Curray, J. R., 2005. Tectonics and history of the andaman sea region, *Journal of Asian Earth Sciences*, **25**(1), 187–228.

Delescluse, M. & Chamot-Rooke, N., 2007. Instantaneous deformation and kinematics of the india-australia plate, *Geophysical Journal International*, **168**(2), 818–842.

Demets, C., 1992a. A test of present-day plate geometries for northeast asia and japan, *Journal of Geophysical Research-Solid Earth*, **97**(B12), 17627–17635.

Demets, C., 1992b. Oblique convergence and deformation along the kuril and japan trenches, *Journal of Geophysical Research-Solid Earth*, **97**(B12), 17615–17625.

Demets, C., Gordon, R. G., Argus, D. F., & Stein, S., 1990. Current plate motions, *Geophysical Journal International*, **101**(2), 425–478.

Demets, C., Gordon, R. G., Argus, D. F., & Stein, S., 1994a. Effect of recent revisions to the geomagnetic reversal time-scale on estimates of current plate motions, *Geophysical Research Letters*, **21**(20), 2191–2194.

Demets, C., Gordon, R. G., & Vogt, P., 1994b. Location of the africa-australia-india triple junction and motion between the australian and indian plates: results from an aeromagnetic investigation of the central indian and carlsberg ridges, *Geophysical Journal International*, **119**(3), 893–930.

DeMets, C., Gordon, R. G., & Royer, J. Y., 2005. Motion between the indian, capricorn and somalian plates since 20 ma: implications for the timing and magnitude of distributed lithospheric deformation in the equatorial indian ocean, *Geophysical Journal International*, **161**(2), 445–468.

Deng, Q. D., Zhang, P. Z., Ran, Y. K., Yang, X. P., Min, W., & Chu, Q. Z., 2003. Basic characteristics of active tectonics of china, *Science in China Series D-Earth Sciences*, **46**(4), 356–372.

DeShon, H. R., Engdahl, E. R., Thurber, C. H., & Brudzinski, M., 2005. Constraining the boundary between the sunda and andaman subduction systems: Evidence from the 2002 m-w 7.3 northern sumatra earthquake and aftershock relocations of the 2004 and 2005 great earthquakes, *Geophysical Research Letters*, **32**(24).

Engdahl, E. R., van der Hilst, R., & Buland, R., 1998. Global teleseismic earthquake relocation with improved travel times and procedures for depth determination, *Bulletin of the Seismological Society of America*, **88**(3), 722–743.

England, P. & Molnar, P., 2005. Late quaternary to decadal velocity fields in asia, *Journal of Geophysical Research-Solid Earth*, **110**(B12), 27.

Feldl, N. & Bilham, R., 2006. Great himalayan earthquakes and the tibetan plateau, *Nature*, **444**(7116), 165–170.

Flesch, L. M., Haines, A. J., & Holt, W. E., 2001. Dynamics of the india-eurasia collision zone, *Journal of Geophysical Research-Solid Earth*, **106**(B8), 16435–16460.

Fournier, M., Chamotrooke, N., Petit, C., Fabbri, O., Huchon, P., Maillot, B., & Lepvrier, C., 2008. In situ evidence for dextral active motion at the arabia-india plate boundary, *Nature Geoscience*, **1**(1), 54–58.

Gan, W. J., Zhang, P. Z., Shen, Z. K., Niu, Z. J., Wang, M., Wan, Y. G., Zhou, D. M., & Cheng, J., 2007. Present-day crustal motion within the tibetan plateau inferred from gps measurements, *Journal of Geophysical Research-Solid Earth*, **112**(B8).

Herring, T. A., 2005. *GLOBK, Global Kalman filter VLBI and GPS analysis program, Version 10.2*, vol. Release 10.2, Mass. Instit. of Tech.

Jade, S., Bhatt, B. C., Yang, Z., Bendick, R., Gaur, V. K., Molnar, P., Anand, M. B., & Kumar, D., 2004. Gps measurements from the ladakh himalaya, india: Preliminary tests of plate-like or continuous deformation in tibet, *Geological Society of America Bulletin*, **116**(11-12), 1385–1391.

Jade, S., Mukul, M., Bhattacharyya, A. K., Vijayan, M. S. M., Jaganathan, S., Kumar, A., Tiwari, R. P., Kumar, A., Kalita, S., Sahu, S. C., Krishna, A. P., Gupta, S. S., Murthy, M., & Gaur, V. K., 2007. Estimates of interseismic deformation in northeast india from gps measurements, *Earth and Planetary Science Letters*, **263**(3-4), 221–234.

Jin, S. G. & Zhu, W. Y., 2003. Active motion of tectonic blocks in east asia: Evidence from gps measurement, *Acta Geologica Sinica-English Edition*, **77**(1), 59–63.

Jolivet, L., Fournier, M., Huchon, P., Rozhdestvenskiy, V. S., Sergeyev, K. F., & Oscorbin, L. S., 1992. Cenozoic intracontinental dextral motion in the okhotsk-japan sea region, *Tectonics*, **11**(5), 968–977.

Kennett, B. L. N. & Widiyantoro, S., 1999. A low seismic wavespeed anomaly beneath northwestern india: a seismic signature of the deccan plume?, *Earth and Planetary Science Letters*, **165**(1), 145–155.

King, R. & Bock, Y., 2005. *Documentation for the GAMIT GPS Analysis software*, vol. Release 10.2, Mass. Instit. of Tech. Scripps Inst.

Oceanogr.

Kogan, M. G. & Steblov, G. M., 2008. Current global plate kinematics from gps (1995-2007) with the plate-consistent reference frame, *Journal of Geophysical Research-Solid Earth*, **113**(B4), 17.

Larson, K. M., Burgmann, R., Bilham, R., & Freymueller, J. T., 1999. Kinematics of the india-eurasia collision zone from gps measurements, *Journal of Geophysical Research-Solid Earth*, **104**(B1), 1077–1093.

Lave, J. & Avouac, J. P., 2000. Active folding of fluvial terraces across the siwaliks hills, himalayas of central nepal, *Journal of Geophysical Research-Solid Earth*, **105**(B3), 5735–5770.

Lepichon, X. & Heirtzle.Jr, 1968. Magnetic anomalies in indian ocean and sea-floor spreading, *Journal of Geophysical Research*, **73**(6), 2101.

McCaffrey, R., Zwick, P. C., Bock, Y., Prawirodirdjo, L., Genrich, J. F., Stevens, C. W., Puntodewo, S. S. O., & Subarya, C., 2000. Strain partitioning during oblique plate convergence in northern sumatra: Geodetic and seismologic constraints and numerical modeling, *Journal of Geophysical Research-Solid Earth*, **105**(B12), 28363–28376.

Meade, B. J., 2007. Present-day kinematics at the india-asia collision zone, *Geology*, **35**(1), 81–84.

Meade, B. J. & Hager, B. H., 2005. Block models of crustal motion in southern california constrained by gps measurements, *Journal of Geophysical Research-Solid Earth*, **110**(B3), –.

Merkouriev, S. & DeMets, C., 2006. Constraints on indian plate motion since 20 ma from dense russian magnetic data: Implications for indian plate dynamics, *Geochemistry Geophysics Geosystems*, **7**, 25.

Paul, J., Burgmann, R., Gaur, V. K., Bilham, R., Larson, K. M., Ananda, M. B., Jade, S., Mukal, M., Anupama, T. S., Satyal, G., & Kumar, D., 2001. The motion and active deformation of india, *Geophysical Research Letters*, **28**(4), 647–650.

Pollitz, F. F., Burgmann, R., & Banerjee, P., 2006. Post-seismic relaxation following the great 2004 sumatra-andaman earthquake on a compressible self-gravitating earth, *Geophysical Journal International*, **167**(1), 397–420.

Prawirodirdjo, L. & Bock, Y., 2004. Instantaneous global plate motion model from 12 years of continuous gps observations, *Journal of Geophysical Research-Solid Earth*, **109**(B8), –.

Prawirodirdjo, L., Bock, Y., McCaffrey, R., Genrich, J., Calais, E., Stevens, C., Puntodewo, S. S. O., Subarya, C., Rais, J., Zwick, P., & Fauzi, 1997. Geodetic observations of interseismic strain segmentation at the sumatra subduction zone, *Geophysical Research Letters*, **24**(21), 2601–2604.

Rao, B. R., 2000. Historical seismicity and deformation rates in the indian peninsular shield, *Journal of Seismology*, **4**(3), 247–258.

Reilinger, R., McClusky, S., Vernant, P., Lawrence, S., Ergintav, S., Cakmak, R., Ozener, H., Kadirov, F., Guliev, I., Stepanyan, R., Nadariya, M., Hahubia, G., Mahmoud, S., Sakr, K., ArRajehi, A., Paradissis, D., Al-Aydrus, A., Prilepin, M., Guseva, T., Evren, E., Dmitrotsa, A., Filikov, S. V., Gomez, F., Al-Ghazzi, R., & Karam, G., 2006. Gps constraints on continental deformation in the africa-arabia-eurasia continental collision zone and implications for the dynamics of plate interactions, *Journal of Geophysical Research-Solid Earth*, **111**(B5).

Replumaz, A. & Tapponnier, P., 2003. Reconstruction of the deformed collision zone between india and asia by backward motion of lithospheric blocks, *Journal of Geophysical Research-Solid Earth*, **108**(B6), 24.

Roy, S. & Rao, R. U. M., 2000. Heat flow in the indian shield, *Journal of Geophysical Research-Solid Earth*, **105**(B11), 25587–25604.

Royer, J. Y. & Gordon, R. G., 1997. The motion and boundary between the capricorn and australian plates, *Science*, **277**(5330), 1268–1274.

Royer, J. Y., Gordon, R. G., & Horner-Johnson, B. C., 2006. Motion of nubia relative to antarctica since 11 ma: Implications for nubia-somalia, pacific-north america, and india-eurasia motion, *Geology*, **34**(6), 501–504.

Sella, G. F., Dixon, T. H., & Mao, A. L., 2002. Revel: A model for recent plate velocities from space geodesy, *Journal of Geophysical Research-Solid Earth*, **107**(B4), –.

Shen, Z. K., Lu, J. N., Wang, M., & Burgmann, R., 2005. Contemporary crustal deformation around the southeast borderland of the tibetan plateau, *Journal of Geophysical Research-Solid Earth*, **110**(B11), 17.

Sieh, K. & Natawidjaja, D., 2000. Neotectonics of the sumatran fault, indonesia, *Journal of Geophysical Research-Solid Earth*, **105**(B12), 28295–28326.

Simons, W. J. F., Socquet, A., Vigny, C., Ambrosius, B. A. C., Abu, S. H., Promthong, C., Subarya, C., Sarsito, D. A., Matheussen, S., Morgan, P., & Spakman, W., 2007. A decade of gps in southeast asia: Resolving sundaland motion and boundaries, *Journal of Geophysical Research-Solid Earth*, **112**(B6).

Socquet, A., Vigny, C., Chamot-Rooke, N., Simons, W., Rangin, C., & Ambrosius, B., 2006a. India and sunda plates motion and deformation along their boundary in myanmar determined by gps, *Journal of Geophysical Research-Solid Earth*, **111**(B5).

Socquet, A., Simons, W., Vigny, C., McCaffrey, R., Subarya, C., Sarsito, D., Ambrosius, B., & Spakman, W., 2006b. Microblock rotations and fault coupling in se asia triple junction (sulawesi, indonesia) from gps and earthquake slip vector data, *Journal of Geophysical Research-Solid Earth*, **111**(B8).

Sol, S., Meltzer, A., Burgmann, R., van der Hilst, R. D., King, R., Chen, Z., Koons, P. O., Lev, E., Liu, Y. P., Zeitler, P. K., Zhang, X., Zhang, J., & Zurek, B., 2007. Geodynamics of the southeastern tibetan plateau from seismic anisotropy and geodesy, *Geology*, **35**(6), 563–566.

Stamps, D. S., Calais, E., Saria, E., Hartnady, C., Nocquet, J. M., Ebinger, C. J., & Fernandes, R. M., 2008. A kinematic model for the east african rift, *Geophysical Research Letters*, **35**(5), 6.

Stein, S. & Gordon, R. G., 1984. Statistical tests of additional plate boundaries from plate motion inversions, *Earth and Planetary Science Letters*, **69**(2), 401–412.

Tapponnier, P. & Molnar, P., 1979. Active faulting and cenozoic tectonics of the tien shan, mongolia, and baykal regions, *Journal of Geophysical Research*, **84**(NB7), 3425.

Thatcher, W., 2003. Gps constraints on the kinematics of continental deformation, *International Geology Review*, **45**(3), 191–212.

Thatcher, W., 2007. Microplate model for the present-day deformation of tibet, *Journal of Geophysical Research-Solid Earth*, **112**(B1), 13.

Wiens, D. A., Demets, C., Gordon, R. G., Stein, S., Argus, D., Engeln, J. F., Lundgren, P., Quible, D., Stein, C., Weinstein, S., & Woods, D. F., 1985. A diffuse plate boundary model for indian-ocean tectonics, *Geophysical Research Letters*, **12**(7), 429–432.

Zhang, P. Z., Shen, Z., Wang, M., Gan, W. J., Burgmann, R., & Molnar, P., 2004. Continuous deformation of the tibetan plateau from global positioning system data, *Geology*, **32**(9), 809–812.

APPENDIX A: FOR AUTHORS

Table **??** is a list of design macros which are unique to GJI. The list displays each macro's name and description.

APPENDIX B: FOR EDITORS

The additional features shown in Table **??** may be used for production purposes.

This paper has been produced using the Blackwell Scientific Publications GJI LaTeX2e class file.

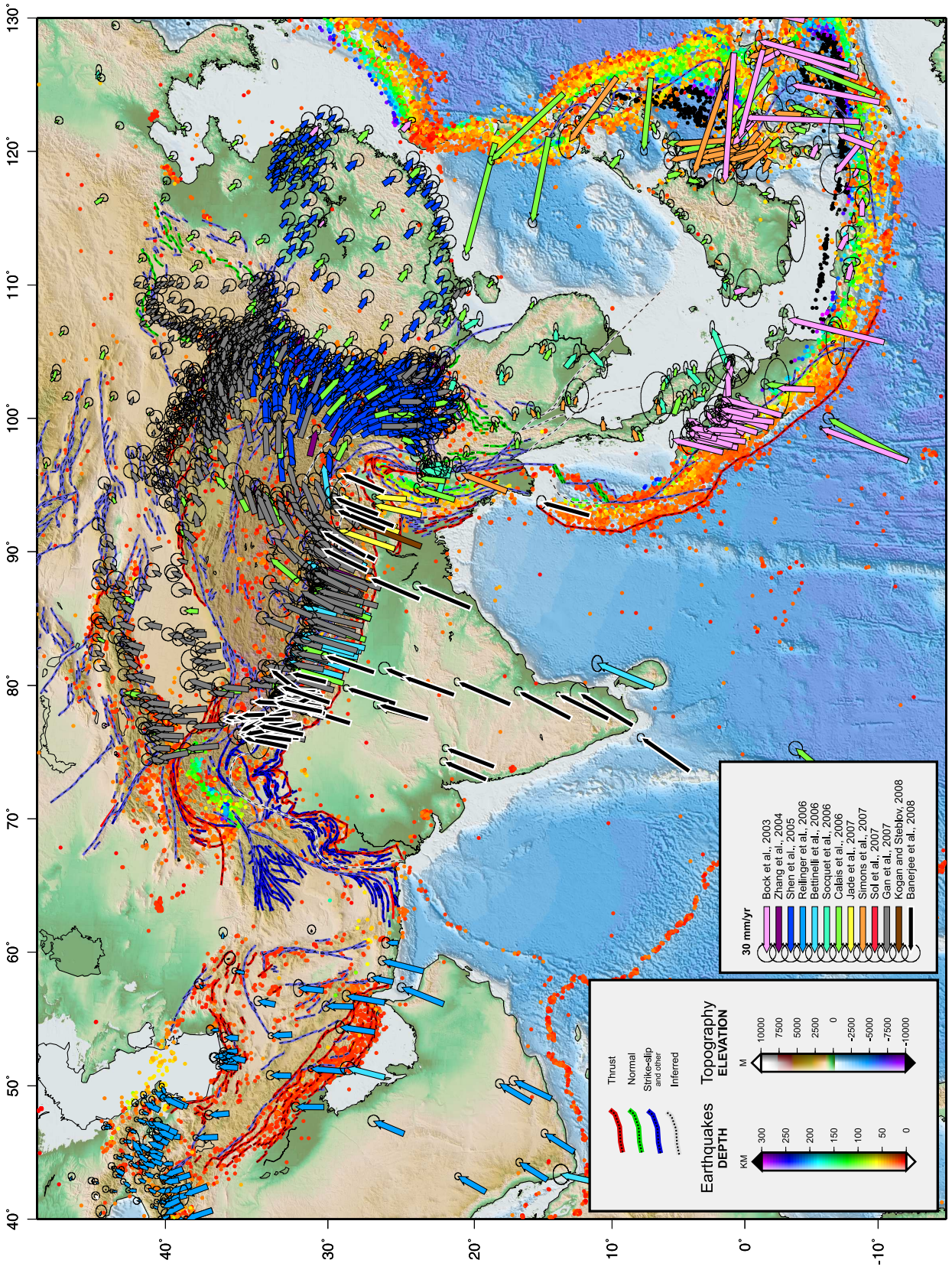
130˚
120˚
110˚
100˚
90˚
80˚
70˚
60˚
50˚
40˚
40˚
30˚
20˚
10˚
0˚
-10˚
30 mm/yr
Bock et al., 2003
Zhang et al., 2004
Shen et al., 2005
Reilinger et al., 2006
Bettinelli et al., 2006
Socquet et al., 2006
Calais et al., 2006
Jade et al., 2007
Simons et al., 2007
Sol et al., 2007
Gan et al., 2007
Kogan and Steblov, 2008
Banerjee et al., 2008
Thrust
Normal
Strike-slip and other
Inferred
Topography ELEVATION
M
10000
7500
5000
2500
0
-2500
-5000
-7500
-10000
Earthquakes DEPTH
KM
300
250
200
150
100
50
0

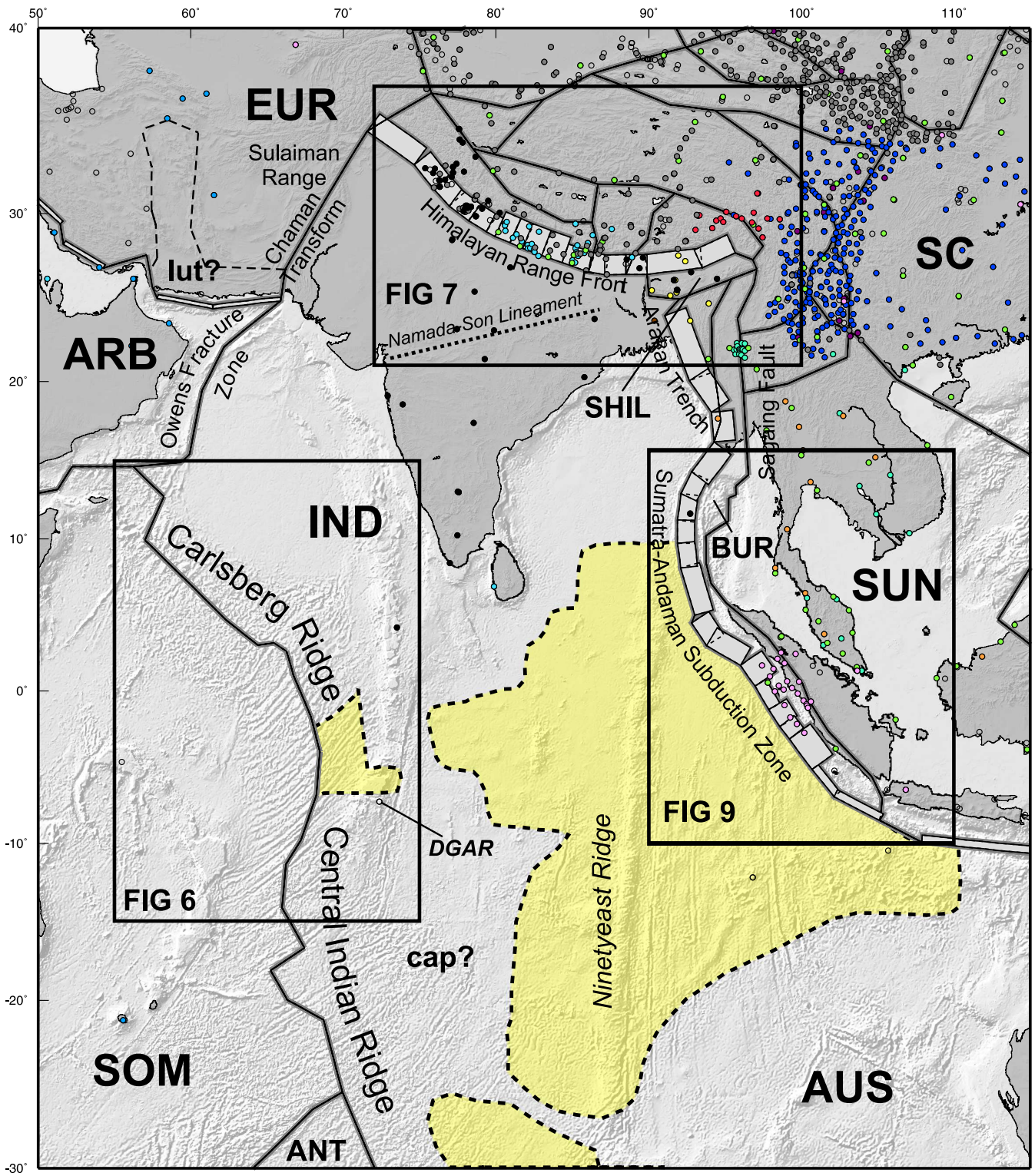

Figure A2. Indian block boundaries used in our block model inversion. Locked portions of dipping fault segments are shaded and shown projected into the horizontal. Circles show the locations of the GPS sites from our combined solution. Filled circles are sites colored by source (see legend in Figure 1) selected from our velocity combination (Figure 1) and used in our inversion (see text for explanation). Zones of diffuse deformation between the Indian and Australian plate are highlighted in yellow (modified from Royer and Gordon, 1997). Rectangular boxes enclose areas of more detailed study. Major blocks (uppercase) and geographic locations mentioned in the text are labeled.

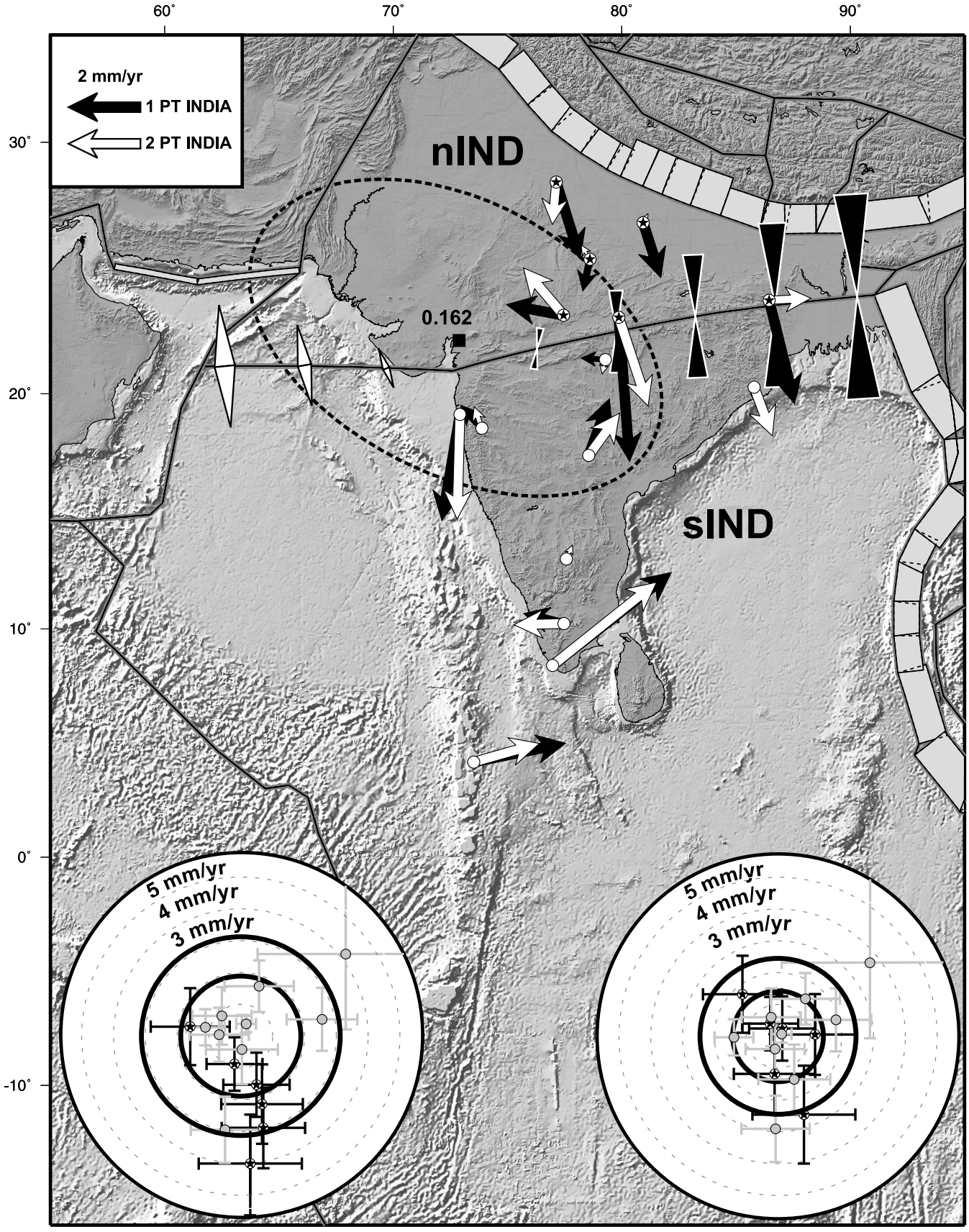

Figure A3. Residual velocities shown for the 1-block India model (black vectors) and the 2-block India model (grey vectors). Separation of the Indian block (grey line) is along the Narmada-Son lineament in central India. The relative pole of rotation for the 2-block India model is shown in the west with a 2-sigma error ellipse. The rotation rate of 0.162 deg/My predicts contraction along the Narmada-Son line from 5 mm/yr in the east to 0 mm/yr near the pole in the west (black triangles). Inset figures show the residual components of the velocities. DGAR is also shown in the inset plot (light grey) but is not used in the Indian plate parameter estimation. Dark concentric circles represent the mean plus 1-sigma uncertainty bounds for misfit values. Sites located north of the

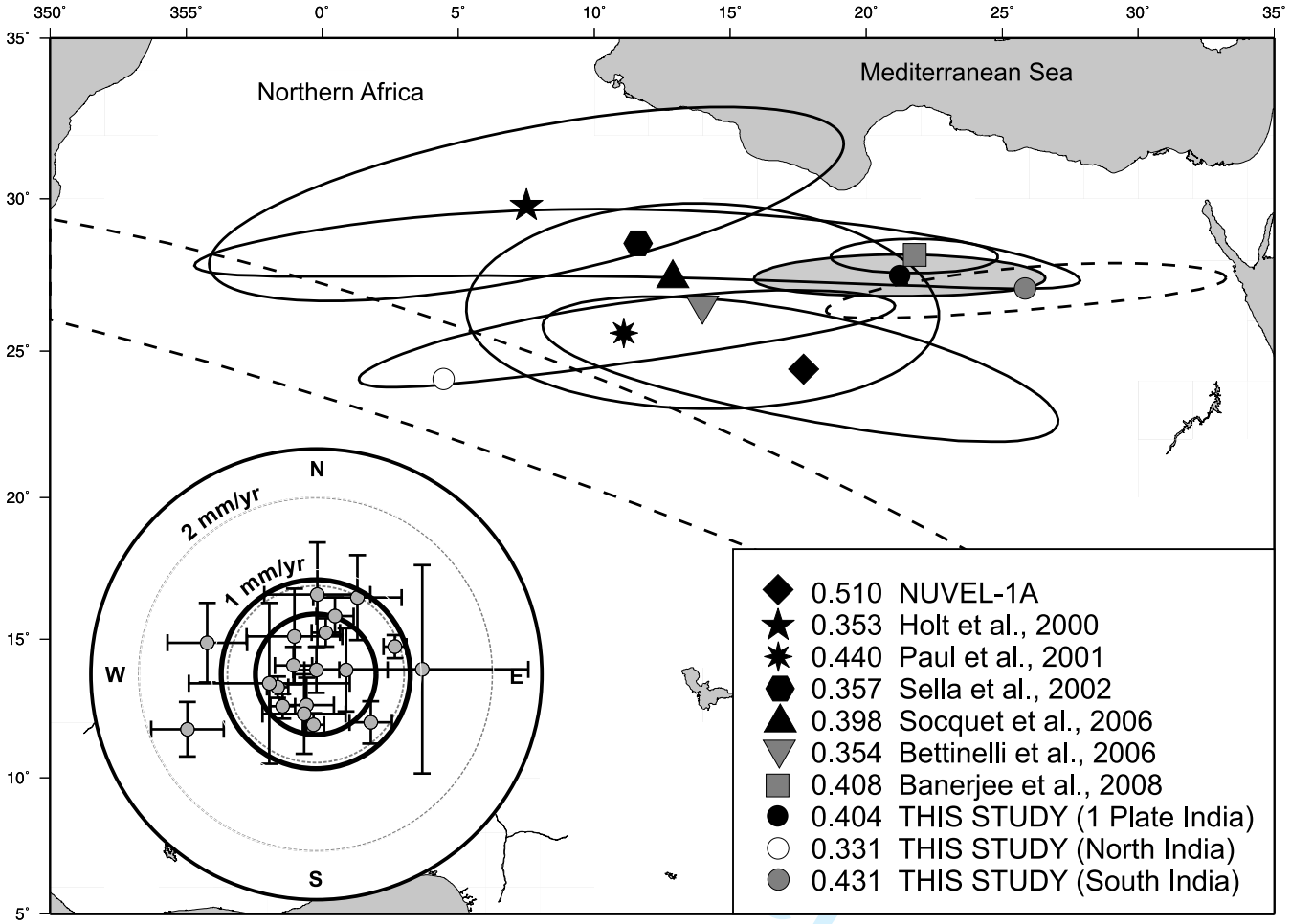

Figure A4. Relative Indian plate poles with respect to Eurasia (see Table 2 for pole details) with 95% confidence ellipses (uncertainties for Socquet et al., 2006a were not reported). The rotation rate (counter-clockwise positive convention) of each pole is shown next to each pole's source in the legend and reported in degrees per million years. We include the IND-EUR pole from our preferred model as well as the nIND-EUR and sIND-EUR poles from our 2-block India model (shaded ellipses). Inset figure shows vector components and 1-sigma error bars of the residual velocities for the stable interior sites of the Eurasian block. All Eurasian residuals are less than 2 mm/yr. Dark concentric circles represent the mean plus 1-sigma uncertainty bounds for misfit values.

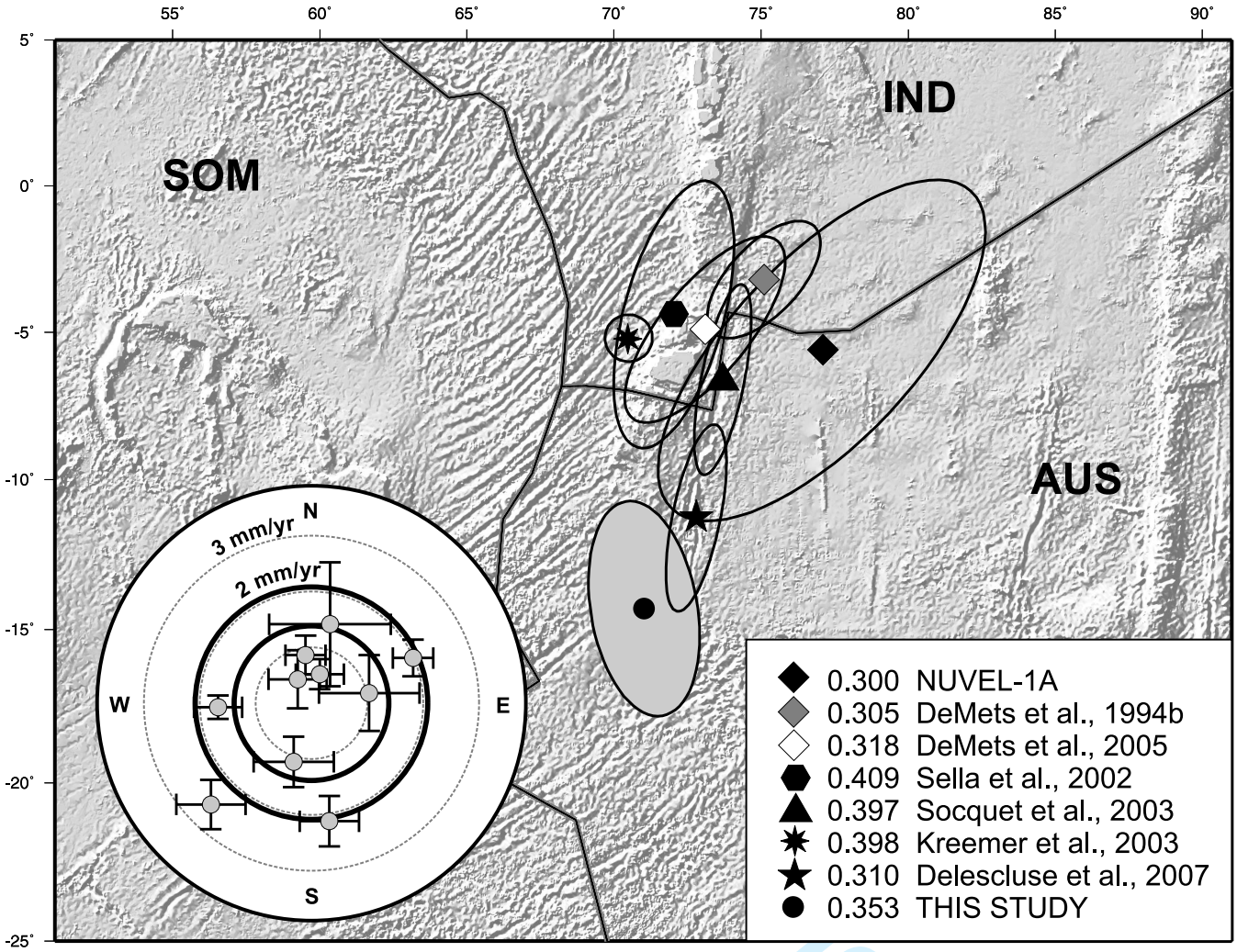

Figure A5. Relative Australian plate poles with respect to India (see Table 2 for pole details) with 95% confidence ellipses. The rotation rate (counter-clockwise positive convention) of each pole is shown next to each pole's source and reported in degrees per million years. Inset figure shows vector components and 1-sigma error bars of the residual velocities for the stable interior sites of the Australian block. DGAR is also shown in the inset plot (light grey) but is not used in the Australian plate parameter estimation. Dark concentric circles represent the mean plus 1-sigma uncertainty bounds for misfit values.

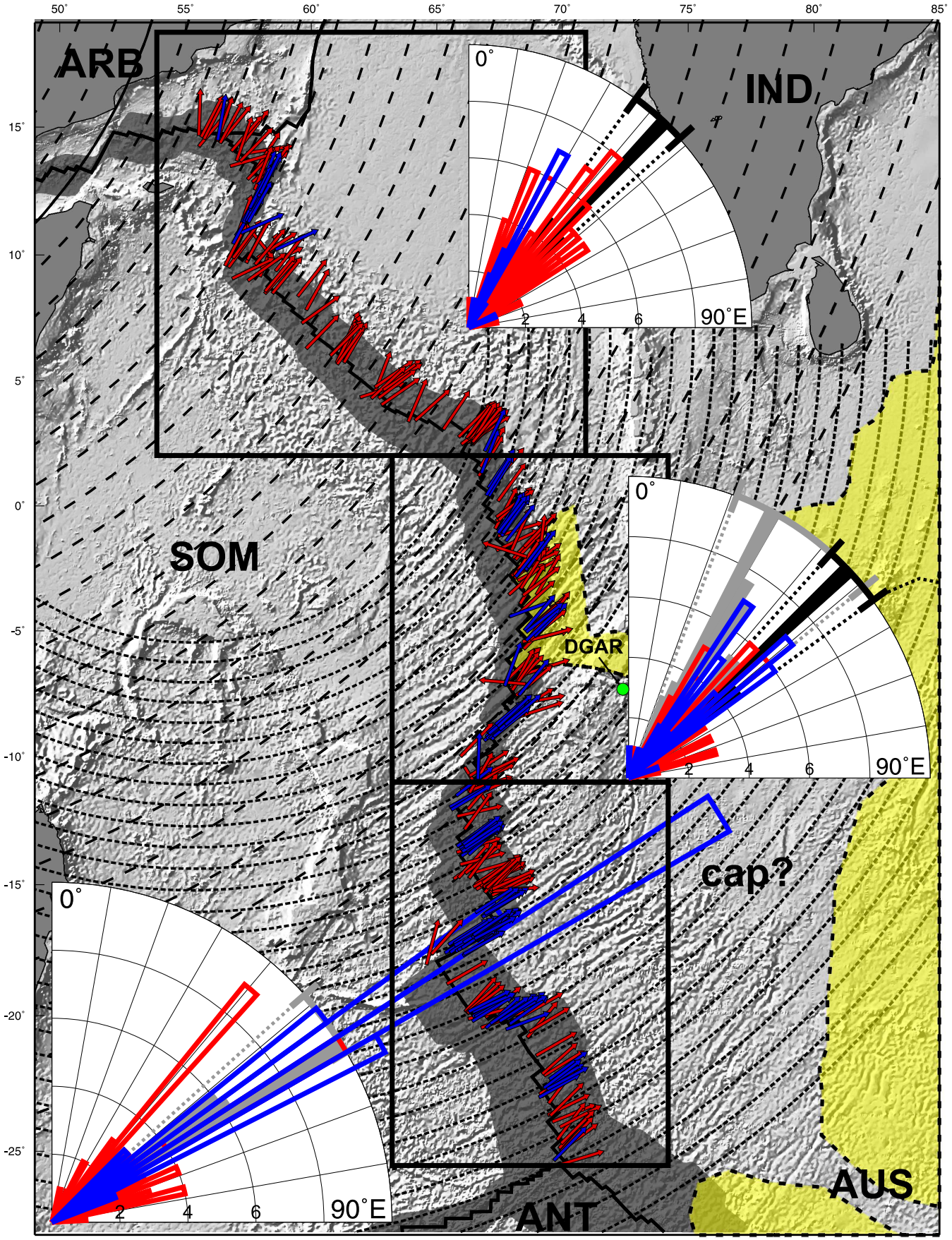

Figure A6. Slip Vectors along the India-Somalia-Australian Plate Boundary Indian-Somalian (Carlsberg Ridge) and Australian-Somalian (Central Indian Ridge) divergent plate boundaries. Oceanic crust from 0-10 Mya is highlighted in grey along the ridges. Small circles represent the predicted relative plate motion direction and displacement rates from our preferred model for both the IND-SOM and AUS-SOM block pairs. The small circles are generally perpen-

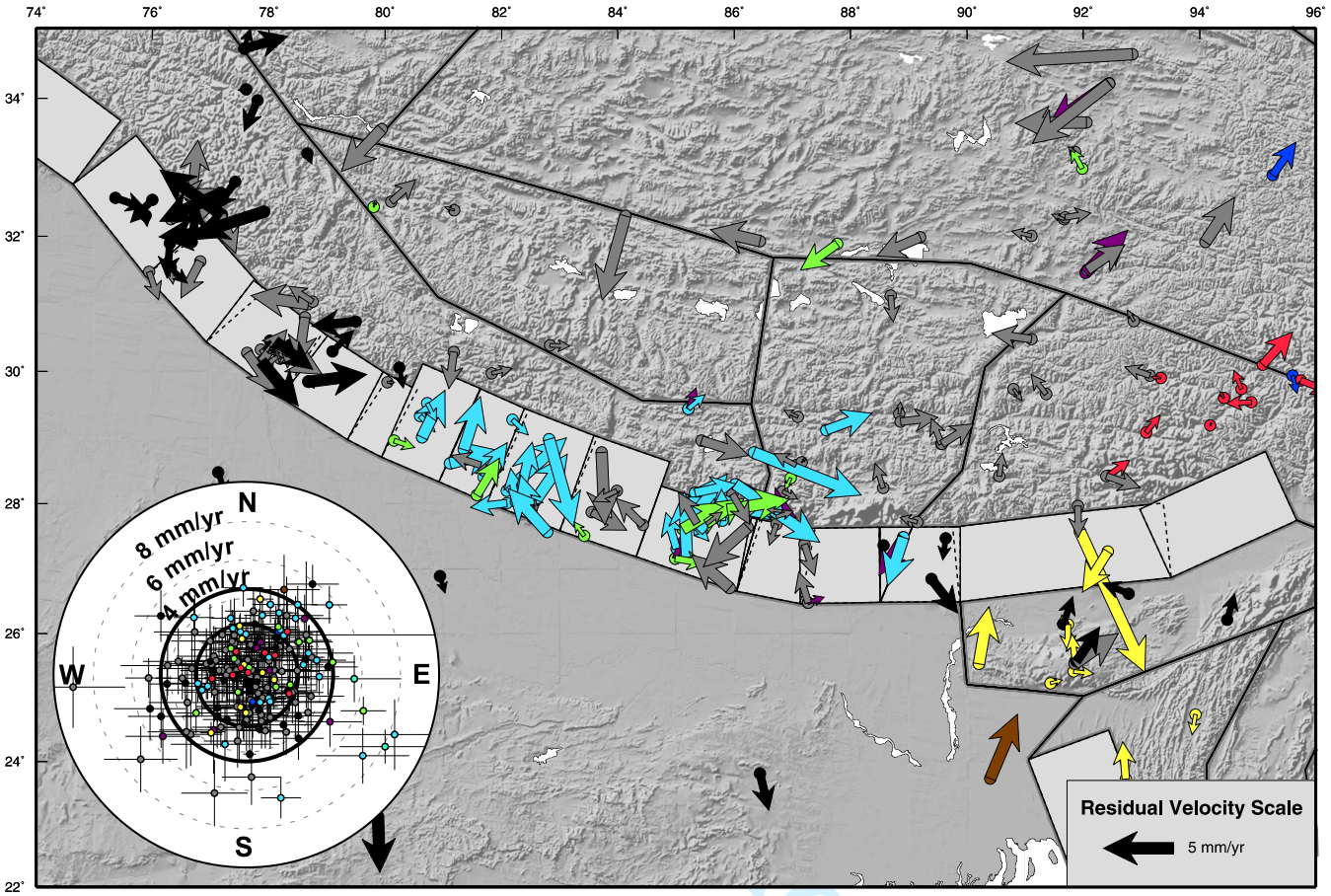

Figure A7. Residual velocities and GPS station locations along the Himalayan range front, sites are colored by source (see legend in Figure 1). Our preferred block model boundaries are shown with dipping segments of the locked portion of the Himalayan thrust faults projected into the horizontal. The 3500-m elevation contour line is also shown for reference. Along the Himalaya fault segments dip at 8 degrees and are locked to 18 km, with the exception of the central HRF. In the central section segment dip shallower at 6 degrees. Inset bull's-eye figure shows the residual velocities for the stations on the map. Dark concentric circles represent the mean plus 1-sigma uncertainty bounds for misfit values.

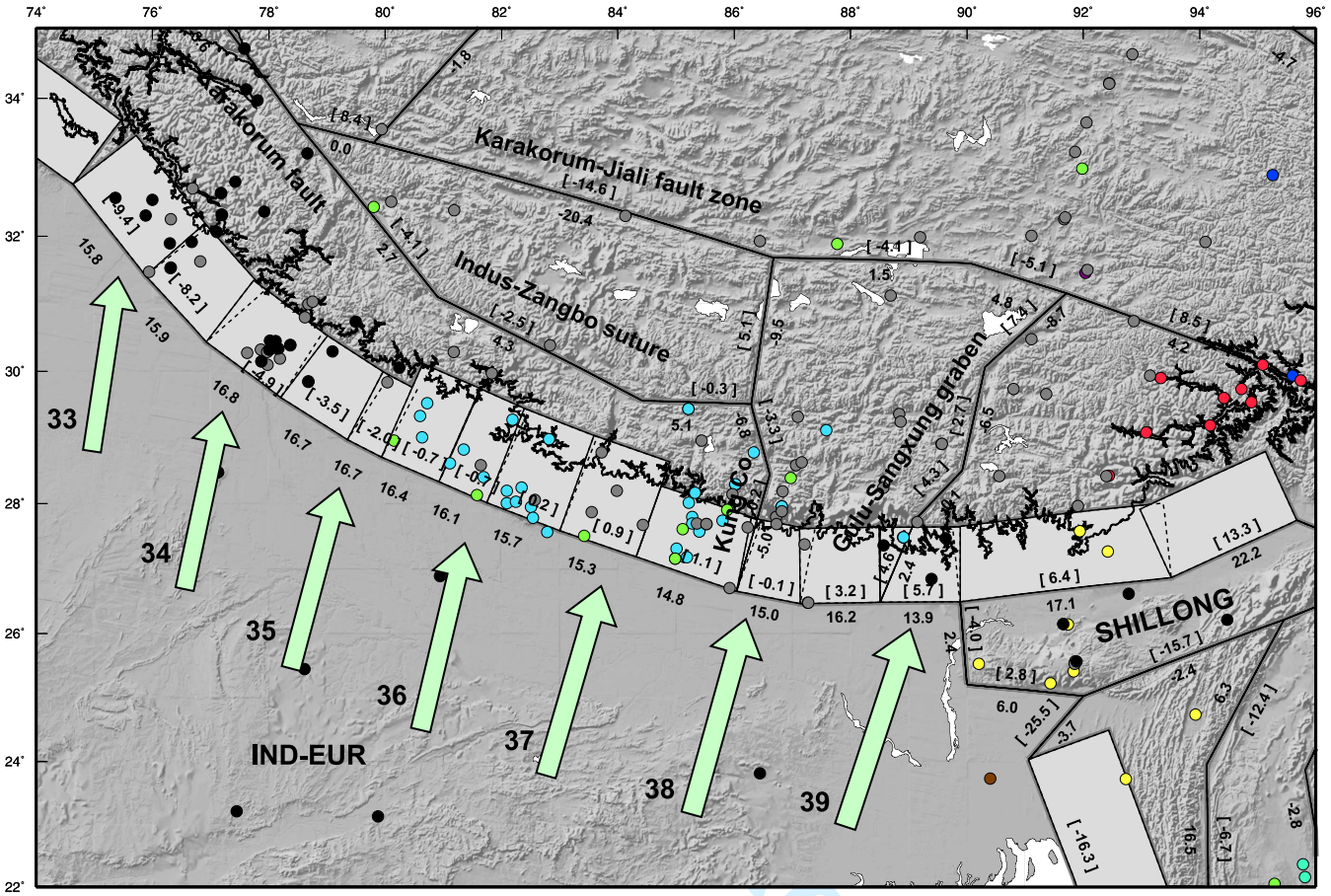

Figure A8. Slip rates and GPS station locations along the Himalayan range front. Our preferred block model boundaries are shown with dipping segments of the locked portion of the Himalayan thrust faults projected into the horizontal. Slip rates in brackets above the fault segments are the strike-slip component with a positive-left lateral convention, dip-slip rates are provided below each segment (thrust motion positive). The 3500-m elevation contour line is also shown for reference. Significant structures and blocks (mentioned in the text) are also labeled. Relative plate motion vectors (IND-EUR) from our preferred model are shown in green. The magnitude of each velocity is shown next to each vector.

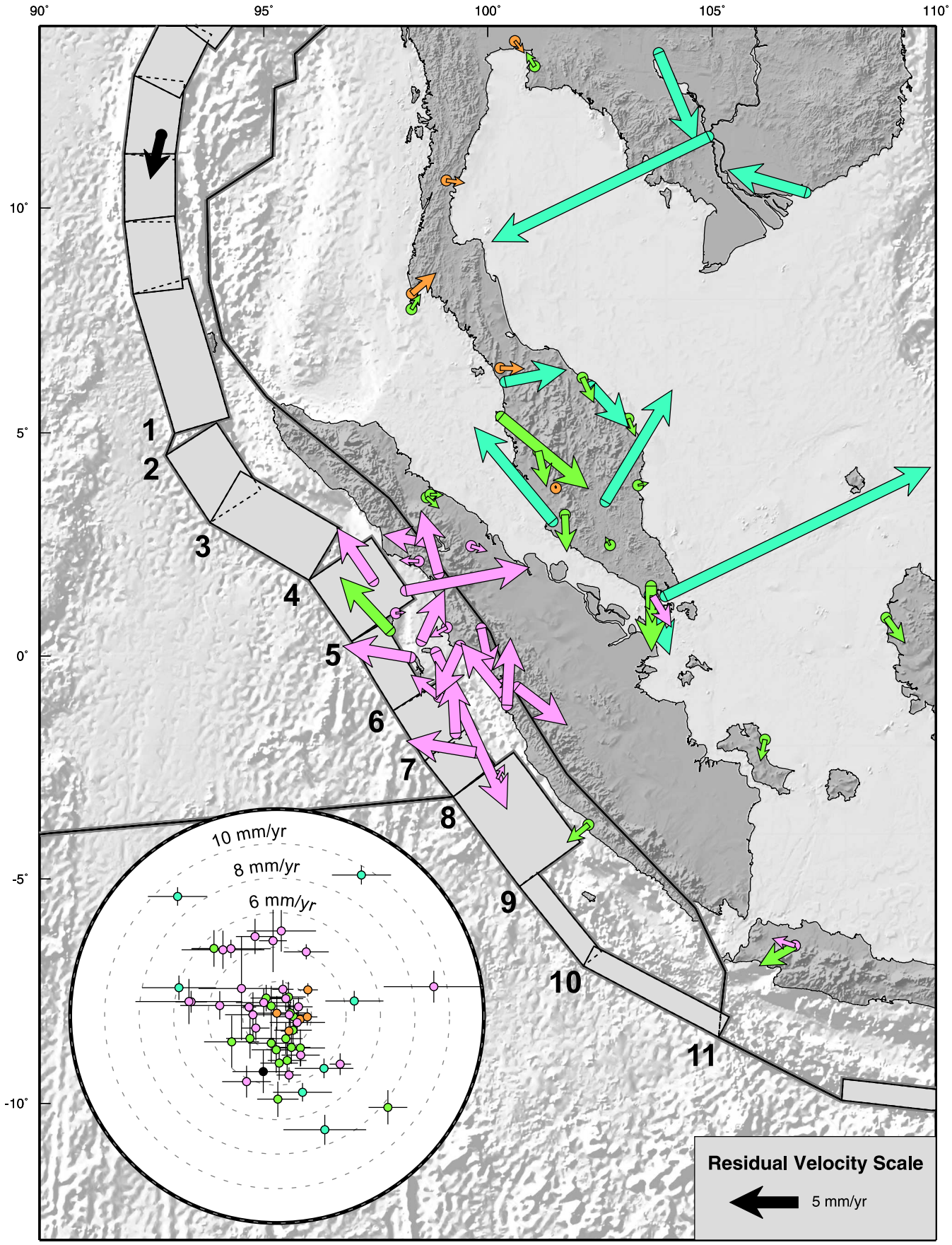

Figure A9. Residual Velocities and GPS station locations along the Sumatra subduction zone and backarc, sites are colored by source (see legend in Figure 1). Our preferred block model boundaries are shown with dipping segments projected to the surface. Slip rates in brackets above the fault segments are the strike-slip component with a positive-left lateral convention, dip-slip rates are provided below each segment (thrust motion positive). Inset bull's-eye figure

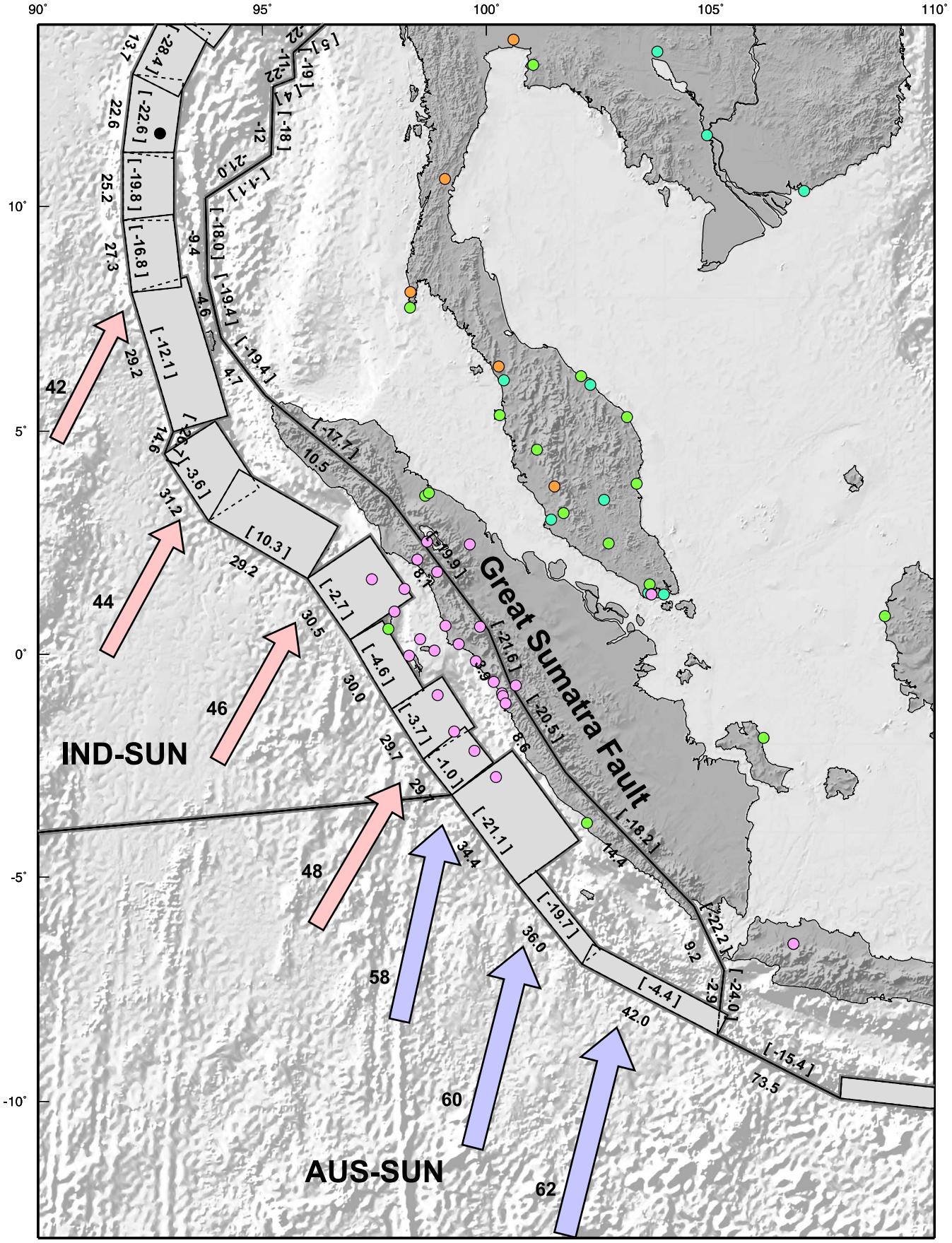

Figure A10. Slip rates and GPS station locations along the Sumatra subduction zone and backarc, sites are colored by source (see legend in Figure 1). Our preferred block model boundaries are shown with dipping segments projected to the surface. Slip rates in brackets above the fault segments are the strike-slip component with a positive-left lateral convention, dip-slip rates are provided below each segment (thrust motion positive). Significant structures and blocks

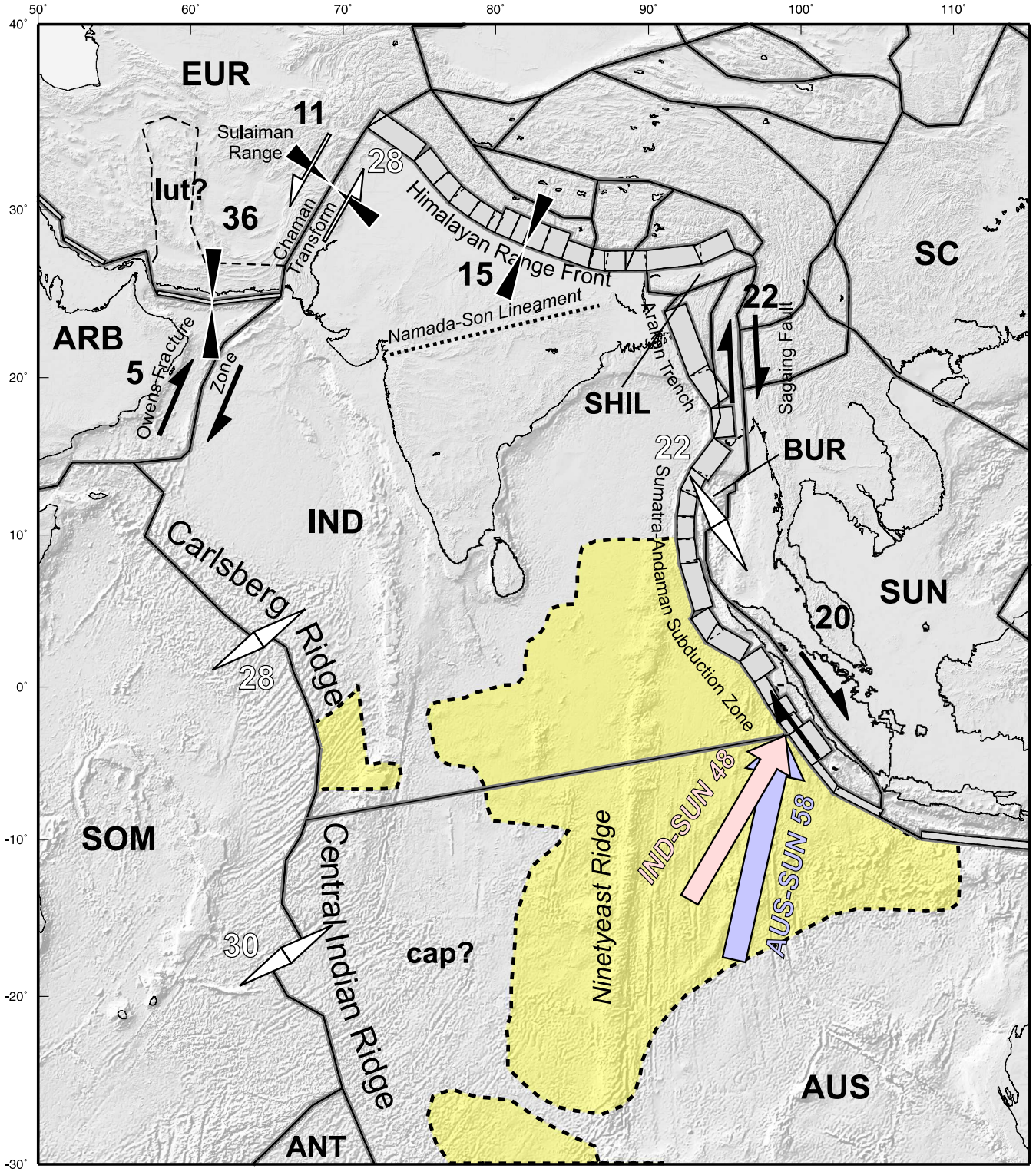

Figure A11. Selected slip rates from our preferred model. Contractional rates are shown by black triangles and extensional rates in white. Dextral rates are shown in black and sinistral rates are shown in white. Indian block boundaries used in our block model inversion are shown with locked portions of dipping fault segments shaded and shown projected into the horizontal. Zones of diffuse deformation between the Indian and Australian plate are highlighted in yellow (modified from Royer and Gordon, 1997). Major blocks (uppercase) and geographic locations mentioned in the text are labeled.

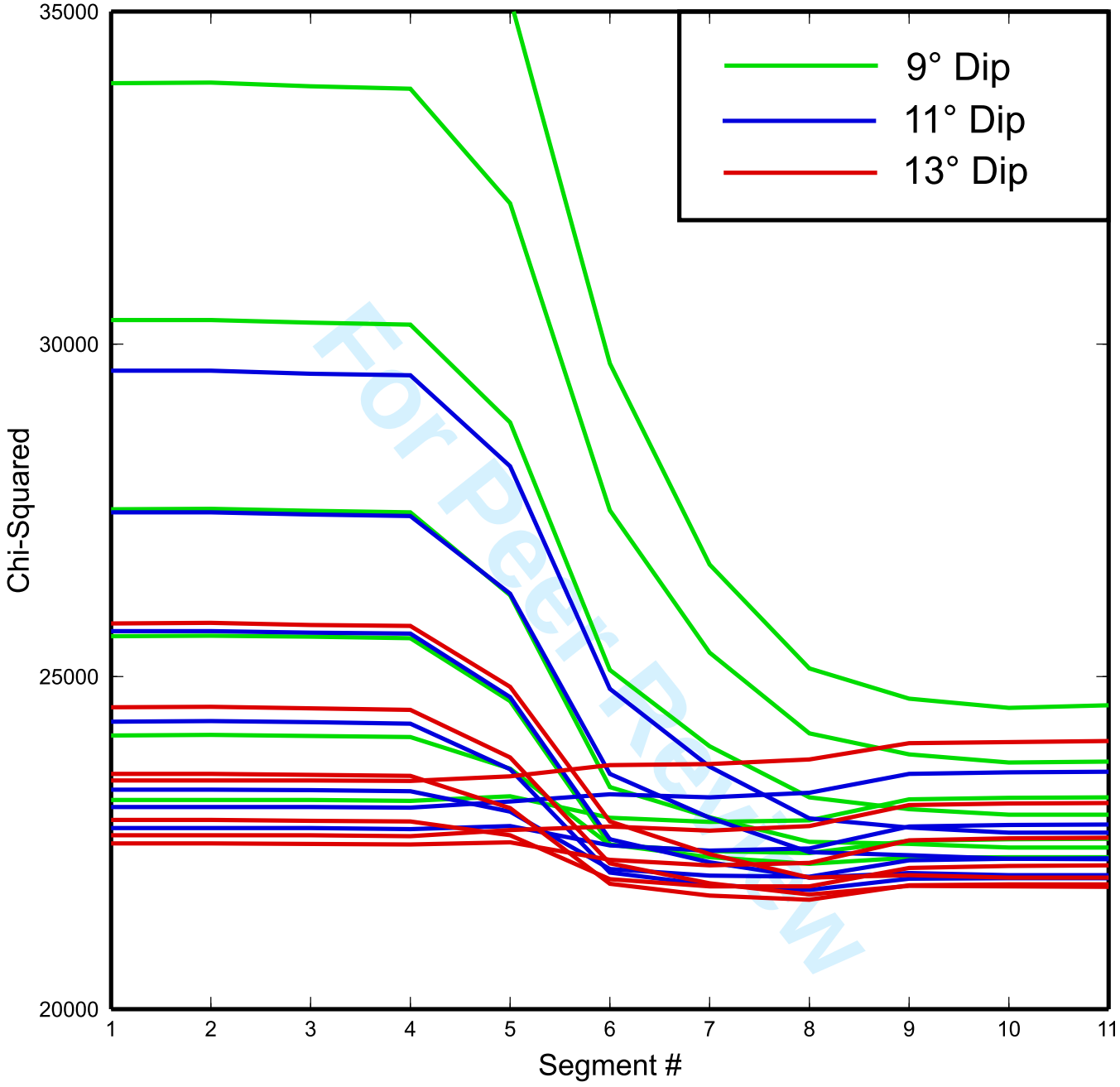

Figure A12. Lines show the value of the misfit statistic (chi-squared) at each segment location (Figure 9) for constant locking depths (20-50 km). Lines are colored by depth.